American Mineralogist, Volume 75, pages 1290–1310, 1990

Nitrogen-defect aggregation characteristics of some Australasian diamonds: Time-temperature constraints on the source regions of pipe and alluvial diamonds

Wayne R. Taylor
Key Centre for Strategic Mineral Deposits, Department of Geology, University of Western Australia, Nedlands 6009, Australia

A. Lynton Jaques
Bureau of Mineral Resources, GPO Box 378, Canberra, ACT 2601, Australia

Michael Ridd
Chemistry Department, University of Tasmania, GPO Box 252C, Hobart, Tasmania 7001, Australia

Abstract

The proportions of aggregated N substitutional defects, platelet intensities, and bulk N contents have been quantitatively determined in type Ia diamonds from the Argyle and Ellendale olivine lamproite pipes (Kimberley block of northwest Australia) and alluvial deposits in western and central Kalimantan (Indonesia) and Copeton (eastern Australia) using Fourier transform infrared (FTIR) microscopy.

The extent of conversion of A defects (a pair of substitutional N atoms) to the aggregated B form is a function of the temperature history, mantle residence time (t_{MR}), and N concentration of diamond. We have used Argyle eclogitic diamonds, which have well-constrained equilibration temperatures (average ≈1255 °C) and short mantle residency (0.4 Ga), together with experimental data to refine the values of the activation energy (E_a) and Arrhenius constant (A) for the A → B reaction. We obtain $E_a/R = 8.16 \pm 0.13 \times 10^4$ K (E_a = 7.03 eV) and ln(A/atomic ppm^{-1} s^{-1}) = 13.51. Kinetic modeling shows that the reaction is sensitive to time-averaged temperatures (designated T_{NA}) in the range 1050–1300 °C and that such temperatures are not necessarily equivalent to those determined by silicate inclusion geothermometry.

The results show that the Ellendale eclogitic diamonds were resident in cool lithosphere and have not experienced the higher temperatures typical of Argyle diamonds. Constraints from inclusion geothermometry indicate that Ellendale eclogitic diamonds must be younger than Argyle diamonds, and a Phanerozoic age is suggested. Copeton diamonds comprise a yellow high-N group (>500 ppm N) and a colorless low-N group (<400 ppm N). They are constrained to a series of moderate temperature isotherms (T_{NA} ≈ 1070–1145 °C, for t_{MR} = 1.6 Ga) and have an extent of N-defect conversion consistent with long-term mantle storage. Remarkably, some of the Kalimantan alluvial and Ellendale peridotitic diamonds lie on the tightly constrained highest temperature (1145 °C) Copeton isotherm, suggesting these diamonds may have had a common origin in ancient Gondwanaland lithosphere that has been dispersed by more recent tectonic processes. A case is made for diamond survival in remnant subcontinental lithosphere underlying southeast Asian and eastern Australian microcontinental blocks that separated from the northeastern Gondwanaland margin during the Paleozoic.

Inasmuch as the N-defect characteristics of diamond reflect a unique mantle thermal history, they may prove useful in provenance studies of alluvial diamonds, in paleotectonic reconstructions, and in deducing the thermal evolution of subcontinental lithosphere, when combined with data from inclusion and xenolith geothermometry.

Introduction

Most natural diamonds (>90%) contain substitutional N impurities in amounts ranging from a few atomic ppm up to ~5000 atomic ppm (Bibby, 1982). Such diamonds are termed type Ia and contain N in lattice defects of two dominant nonparamagnetic types: the A defect, which is a pair of substitutional N atoms, and the B-defect, which consists of four N atoms arranged tetrahedrally about a vacancy (Bursill, 1983; Bursill and Glaisher, 1985). A and B defects and a third defect of uncertain structure known as D give rise to characteristic infrared (IR) ab-

0003–004X/90/1112–1290$02.00

sorptions from which the quantitative proportions of each defect type can be determined (Davies, 1981; Clark and Davey, 1984a; Woods, 1986).

Experimental work at high pressures and temperatures (Allen and Evans, 1981; Evans and Qi, 1982) has shown that A defects combine to form B defects in measurable amounts at temperatures >2400 °C for experiment times of ~1 h. Evans and Qi calculated an activation energy for this process and showed that at upper mantle temperatures the A → B conversion will take place on reasonable geological time scales. Subsequently, Evans and Harris (1989) modeled the reaction kinetically and showed that the relative proportion of A and B defects can be used to provide an estimate of the diamond storage temperature in the mantle or the mantle residence time of diamond. Evans and Harris pointed out, however, that a more precise calibration of the kinetic equations was required before the technique could be reliably used as a geothermometer or geochronometer.

Sequence of N aggregation

Experimental studies have shown that the A → B aggregation reaction is part of an overall aggregation sequence that begins with the incorporation of singly substituted N, as point defects, into the diamond structure during diamond growth in the mantle (Dyer et al., 1965; Chrenko et al., 1977). Diamonds with an abundance of singly substituted N atoms are known as type Ib; most synthetic diamonds are of this type. During high temperature annealing the singly substituted N atoms migrate and combine to form the more stable A defects, comprising a pair of N atoms on adjacent sites (Davies, 1976). Further aggregation results in the formation of B defects, or aggregates of four N atoms and a vacany (Evans and Harris, 1989). Associated with B-aggregate formation is the concurrent production of larger planar structures known as platelets, which are identifiable by their characteristic B′ localized mode IR absorption. In addition to these dominant aggregations, a minor side reaction in the A → B aggregation process may produce N3 centers (a paramagnetic defect consisting of three N atoms and a vacancy). N3 centers impart a characteristic yellow color in B-defect-rich diamonds of high N content (Harris, 1987).

Platelets may ultimately degrade to form a diamond with pure B character or may undergo catastrophic degradation, forming dislocation loops, which results in platelet-depleted diamonds containing mixed A and B defects (Woods, 1986). Diamonds that show platelet degradation have been termed irregular by Woods (1986), whereas those in which the reaction A → B + platelets has proceeded in a smooth fashion have been termed regular. Among diamonds from the Argyle mine, Harris and Collins (1985) have recognized that a high proportion of the eclogitic diamonds are platelet-degraded—a feature that is, at present, apparently unique to the Argyle diamond population and suggests an atypical mantle history compared with other diamond provinces worldwide.

There has been considerable controversy concerning the structure, chemical composition, and mechanism of degradation of platelets (Lang, 1979; Humble, 1982; Barry et al., 1985; Bursill and Glaisher, 1985; Woods, 1986). Although many authors have assumed that platelets are N rich, recent IR spectroscopic data (Woods, 1986) support the view that platelets are largely carbonaceous defects and actually contain little N. The strong B′ IR absorption at ≈1370 cm^{-1} has been assigned by Woods to the stretching vibration of C-C bonds within the platelet.

Diamond source regions in the upper mantle

There has been much interest in defining the P, T, f_{O_2}, and age of diamond source regions in the upper mantle. Haggerty (1986) presented a detailed model for the structure of the subcontinental lithosphere and suggested that B-defect-rich type Ia diamonds will predominate among eclogitic source rocks at the base of the lithosphere, whereas A-defect-rich diamonds will be prevalent in the cooler interior of the lithosphere where peridotites will be the major host. Haggerty further suggested that type II diamonds (which have essentially no IR-active substitutional N) will be mainly found in eclogitic, N-depleted mantle, and type Ib diamonds will be restricted to the uppermost interior of the lithosphere. Although this conceptual model offers a starting point for understanding diamond distribution in the upper mantle, it is based on an assumed thermal structure for the lithosphere and asthenosphere (derived mainly from xenolith and diamond inclusion geothermobarometry) and on the assumption of generally old Archean ages (>3 Ga) for macrodiamonds. Furthermore, recent studies of peridotitic and eclogitic diamonds from the Finsch and Premier pipes (Deines et al., 1989) have demonstrated that type II diamonds can occur in both the eclogitic and peridotitic parageneses, and in certain pipes may be more common among peridotitic paragenesis diamonds. Deines et al. (1989) also showed that eclogitic diamonds from the same pipe may have a wide range of N contents and aggregation states.

It is now known from isotopic dating studies that diamond formation is not restricted to the Archean. Diamonds of the eclogitic paragenesis, in particular, appear to have largely formed beneath cratonic regions during the Proterozoic (Kramers, 1979; Richardson, 1986; Smith et al., 1989; Phillips et al., 1989), and in some cases multiple episodes of diamond formation are indicated. Since the extent of A → B conversion in type Ia diamonds is sensitive to residence time in the mantle as well as temperature and total N content (Evans and Harris, 1989), correlation of the proportion of A or B defects with the depth of the diamond source region as suggested by Haggerty (1986) is not straightforward. Furthermore, if there are multiple source regions for diamond sampled by the same kimberlite or lamproite pipe, then the statistical validity in characterizing the diamond source by silicate inclusion geothermobarometry, which necessarily can only involve a small percentage of the diamond population,

may be questionable. This has been recognized by Deines et al. (1989), who have identified several distinct populations among Finsch and Premier diamonds and therefore caution against generalized interpretations of diamond source regions where commonality of origin of a diamond suite cannot be assured. A preferable approach would be to use diamond N aggregation characteristics, which can be determined on any transparent type Ia sample by IR spectroscopy, to discriminate diamonds from different mantle source regions on the basis of their time-temperature history. From these populations diamonds could then be selected for age dating and geothermobarometry. For alluvial diamonds it is conceivable that their N aggregation state could be used to identify the number of contributing sources and, in favorable cases, diamond provenance could be determined. In this paper these concepts have been applied in an attempt to define mantle conditions for diamonds from known sources and to identify the provenance of diamonds from alluvial sources.

To assess the applicability of N aggregation in characterizing diamond source regions and evolutionary history, we have measured the Fourier transform infrared (FTIR) spectra of diamond samples from well-known lamproite pipe occurrences in the Kimberley region of northwest Australia (Argyle, Ellendale-4, and Ellendale-9 pipes) and alluvial occurrences in Kalimantan (approximately 2000 km to the northwest of the Kimberley block) and Copeton in eastern Australia (about 800 km to the east of the inferred Precambrian boundary in eastern Australia). Because the alluvial diamonds occur in Paleozoic to Mesozoic terranes in areas remote from stable cratonic nuclei and occur in sufficient abundance to suggest local provenance (MacNevin, 1977; Bergman et al., 1988), the nature of their diamond source regions is of considerable interest.

Our approach is to refine the calibration of the kinetic equations for the A → B aggregation reaction and better quantify the relationships among aggregation state, time, temperature, and other variables. We then consider in detail the N aggregation characteristics of a data set containing 49 diamonds described below.

Sample description and localities

Argyle diamonds

The Argyle (AK1) pipe in the East Kimberley region is the world's largest producer of diamonds, 34.6 million carats were mined in 1988. Rb-Sr and K-Ar dating indicate an emplacement age of 1.18 Ga for the Argyle pipe (Pidgeon et al., 1989). Argyle diamonds are mostly small (mean size <0.1 carat) and brown in color, and are typically strongly frosted, plastically deformed, resorbed dodecahedra (Hall and Smith, 1984). Primary inclusions within the Argyle diamonds are overwhelmingly of eclogitic paragenesis, with orange garnet being the most common, followed by omphacite, coesite, rutile (Nb-Zr bearing), sulfide (FeS), kyanite, and, rarely, Mg-poor ilmenite and moissanite (α-SiC) (Jaques et al., 1989). Many stones contain multiple inclusions, garnet + coesite ± omphacite being relatively common.

Ten type Ia eclogitic diamonds from Argyle were included in the data set. Seven of these, six with A*nn* series sample numbers, and diamond AA17 have been documented in terms of their color, morphology, inclusion mineralogy, and C isotopic composition in Table 8 of Jaques et al. (1989). Trace-element concentrations in the mineral inclusion suite of both Argyle and Ellendale diamonds, determined by proton microprobe, have been presented by Griffin et al. (1988). The remaining samples (A200 series) are pale brown octahedra or pale yellow dodecahedra with numerous eclogitic inclusions. Rare peridotitic paragenesis diamonds (~5% of the population) are also present in the Argyle commercial population but were not sampled in this study. These are sharp-edged planar octahedral diamonds with etched and frosted surfaces similar to those found within peridotite xenoliths from the Argyle pipe (Hall and Smith, 1984; Jaques et al., 1990).

Ellendale lamproite pipes 4 and 9

The diamondiferous Ellendale olivine lamproites form part of the West Kimberley lamproite province, which comprises more than 100 intrusions, all of Miocene age (18–22 Ma), located at the northern margin of the Canning Basin and southern flank of the Kimberley block (Atkinson et al., 1984; Jaques et al., 1984, 1986). Ellendale pipes 4 and 9 have the highest diamond grades of the West Kimberley lamproites: 14 and 5 carats/100 metric tons, respectively.

Ellendale stones have a distinctive appearance (Hall and Smith, 1984). Commercial-sized stones (>1 mm) are typically yellow, resorbed, rounded dodecahedra with lustrous, smooth surfaces. A high proportion (60–90%) are of gem quality. Below 1 mm the dominant crystal form is a planar, step-layered, frosted octahedron, either colorless or pale brown. Diamonds from Ellendale pipes 4 and 9 contain approximately equal proportions of peridotitic and eclogitic inclusions (Jaques et al., 1989).

Three eclogitic diamonds from the Ellendale-4 and two diamonds from the Ellendale-9 olivine lamproite pipes were included in the data set (Table 1). Silicate inclusions indicate that one of the Ellendale-9 diamonds (E9/9) is peridotitic, whereas the other (E9/16) is of uncertain paragenesis. This latter diamond, however, has a $\delta^{13}C$ value of −6.4‰, close to the −5.7‰ average of other Ellendale peridotitic suite diamonds (Jaques et al., 1989), and therefore it can be confidently assumed also to be peridotitic. Full details of the stones included in this data set are given in Table 2.7 of Jaques et al. (1989).

Copeton alluvial diamonds

More than 200 000 carats of alluvial diamonds are recorded as having been produced from the Copeton area of New South Wales, mostly between 1871 and 1920, but actual production could have been significantly higher (MacNevin, 1977; Lishmund and Oakes, 1989).

TABLE 1. Results of diamond IR spectral decomposition

Sample no.	Color	3107 cm^{-1} H defect	N(tot) atomic ppm	A defect percent	μ (A) cm^{-1}	μ (B) cm^{-1}	μ (D) cm^{-1}	μ (T) cm^{-1}	I (B') cm^{-2}	T (NA)* (°C)
Copeton										
CO1	CL	–	93	96	26.87	0.44	0.00	27.31	3.7	1094
CO4	CL	–	55	99	16.26	0.05	0.00	16.32	1.1	1071
CO5	CL	–	203	77	46.73	4.62	0.42	51.76	37.1	1123
CO6	CL	–	105	92	28.80	1.04	0.00	29.84	7.7	1110
CO8	CL	–	166	58	28.95	4.97	1.38	35.30	28.7	1149
CO9	CL	–	309	50	45.90	10.45	3.45	59.79	53.2	1142
CO10	CL	–	41	99	12.02	0.06	0.00	12.08	0.9	1085
CO11	CL	–	363	45	49.24	12.96	4.54	66.75	82.0	1143
CO13	BR	+	182	83	45.44	3.12	0.22	48.78	24.4	1116
CO14	CL	–	283	48	40.92	9.97	3.17	54.06	60.6	1146
CO17	Y	+	630	48	90.00	21.60	7.50	119.10	132.0	1127
CO18	CL	–	68	95	19.33	0.44	0.00	19.77	3.9	1109
CO20	CL	+	111	86	28.80	1.80	0.00	30.60	12.8	1122
CO21.1	Y	+	1015	32	98.40	68.28	5.90	172.58	o.s.	1131
CO21.2	Y	+	945	33	93.30	66.48	4.00	163.78	o.s.	1132
CO26	CL	–	150	77	34.49	3.33	0.36	38.17	23.9	1130
CO27	CL	–	64	99	19.15	0.06	0.00	19.21	1.4	1065
CO28	Y	+	773	35	81.39	51.12	3.80	136.31	o.s.	1134
CO29	CL	–	159	85	40.53	1.96	0.38	42.86	15.6	1116
CO30	CL	–	20	>99	5.87	<0.03	0.00	5.90	0.0	<1100
CO31	Y	–	568	49	83.19	22.28	5.26	110.73	o.s.	1128
CO32	CL	–	279	72	60.02	8.02	0.61	68.65	47.8	1122
CO33	CL	–	49	99	14.62	0.06	0.00	14.68	2.1	1076
CO34	BR	–	202	74	45.20	5.26	0.39	50.85	27.3	1126
CO35	CL	–	80	82	19.67	1.30	0.19	21.16	6.8	1141
CO36	CL	–	60	95	17.03	0.34	0.00	17.36	3.2	1109
CO37	CL	–	167	74	36.80	3.94	0.55	41.29	26.7	1132
CO39	Y	+	1220	48	171.00	69.60	3.50	244.10	o.s.	1112
DA101	CL	–	140	85	35.80	1.75	0.29	37.84	16.0	1118
DA122	CL	–	80	95	22.75	0.48	0.00	23.23	6.4	1104
DA131	CL	–	237	54	38.49	8.00	2.10	48.59	43.3	1144
Argyle										
A19	BR	+	63	5	0.98	6.18	0.42	7.58	4.4	1303
A25	BR	+	19	39	2.23	1.38	0.00	3.61	0.2	1265
A26	BR	+	42	23	2.87	3.12	0.32	6.31	4.1	1264
A27	BR	+	10	42	1.26	0.69	0.00	1.95	0.8	1280
A47	BR	+	69	14	2.85	5.53	0.69	9.07	11.0	1268
AA17.1	BR	+	57	28	4.80	4.19	0.32	9.32	8.9	1248
AA17.2	BR	+	57	26	4.50	4.20	0.34	9.03	8.4	1250
AA17.3	BR	+	66	34	6.60	4.56	0.28	11.43	15.0	1236
AA17.4	BR	+	70	27	5.70	5.64	0.20	11.55	14.7	1243
A201	Y	+	65	41	8.00	4.01	0.24	12.25	14.0	1228
A202	BR	+	78	14	3.35	6.87	0.46	10.68	11.7	1263
A203	BR	+	37	15	1.67	3.22	0.25	5.13	3.7	1283
A204	Y	+	206	21	12.93	14.70	2.01	29.64	45.4	1223
Ellendale-4										
E4/3	CL	+	631	95	179.36	3.50	0.20	183.06	31.9	1059
E4/7.1	CL	–	480	95	136.57	2.91	0.00	139.48	29.1	1064
E4/7.2	CL	–	409	95	117.00	2.28	0.00	119.28	31.0	1065
E4/14	CL	–	218	96	62.97	1.02	0.00	63.99	6.5	1075
Ellendale-9										
E9/9	CL	–	133	67	26.49	3.79	0.63	30.91	19.0	1146
E9/16	CL	+	379	2	2.11	25.58	7.94	35.63	106.0	1241
Kalimantan										
KAL1	Y	–	79	75	17.69	2.02	0.14	19.85	10.4	1148
KAL2	BR	+	41	87	10.76	0.62	0.00	11.39	1.2	1144
KAL4	Y	–	298	7	6.31	23.84	3.90	34.04	50.5	1209
KAL5	BR	+	125	72	26.98	3.45	0.30	30.73	16.1	1141

Note: o.s. = off-scale, + = present, – = absent, CL = colorless, BR = pale brown to brown, Y = pale yellow to yellow.
* N aggregation temperatures calculated using t_{MR} = 1.6 Ga for CO, E4, E9, and KAL diamonds, and t_{MR} = 0.4 Ga for Argyle diamonds.

The source of the diamonds is unknown; a number of local sources seems likely on the basis of the differing characteristics of stones from different localities (MacNevin, 1977), with the source pipe or pipes perhaps buried beneath thick Tertiary basalt flows. The Copeton stones are notable for their multiple twinning, which makes them unusually hard to cut (Joris, 1983). Other characteristics of the Copeton stones are a predominance of eclogitic paragenesis diamonds (>80%) with unusually heavy $\delta^{13}C$ values and an inclusion suite in which coesite- and grossular-rich garnets are conspicuous (Sobolev, 1984).

In this study 39 Copeton diamonds (CO and DA series) were examined. Most are macles with the dodecahedron

form, and about a third are pale yellow in color, with the remainder being colorless to very pale brown. Common surface features include etch pits and channels, striations, and glide lines; some stones have lightly frosted surfaces and some have green spots caused by radiation damage.

Kalimantan alluvial diamonds

Alluvial diamonds have previously been reported from three provinces in Kalimantan: the Landak River region of west Kalimantan, the Barito province of central Kalimantan, and in the Meratus Range area of southeast Kalimantan, but their primary sources are unknown (e.g., Bardet, 1977; Bergman et al., 1988). The Pamali breccia at the southern end of the Meratus Range was thought by early workers (see Bardet, 1977) to be a kimberlite and the Borneo-type source rock for the alluvial diamonds. However, the Pamali breccia has recently been reinterpreted as a sedimentary conglomerate derived from local ophiolite complexes (Bergman et al., 1987).

We have studied two stones purchased from a local dealer in Ngabang close to the workings in the Landak region (KAL1, KAL2), and two more (KAL4, KAL5) were obtained from a prospect on the Keliam River, a tributary of the Mahakam River, located approximately 150 km northwest of the Barito diamond province. KAL1 and 2 are pale yellow and brown dodecahedra, respectively, with chips and surface cracks (KAL1) suggesting an extensive alluvial history, whereas KAL4 and KAL5 are, respectively, a pale yellow octahedron and a pale brown dodecahedron with smooth surfaces and fine striations.

Experimental

IR spectra acquisition

IR spectra of the diamond samples were recorded over the range 4000–450 cm^{-1} on a Digilab FTS-20E FTIR spectrometer using a Digilab UMA-100 IR microscope accessory equipped with a liquid-N_2-cooled MCT detector. Spectra were recorded in transmission mode at a resolution of 4 cm^{-1} by averaging the signals of ~100 scans. Diamond samples, as fragments, plates, or rough stones of ~0.5–4.0 mm thickness, were mounted directly on a variable aperture diaphragm, and spectra were obtained on areas 250 μm in diameter. For irregularly shaped specimens, spectra were recorded at the point of maximum light transmission through the sample.

For quantitative measurement of the N content, the optical path length of transmitted radiation through the diamond sample must be accurately determined. In planar sections with parallel sides this is simply achieved by measuring the specimen thickness. In nonplanar stones determination of path length is not straightforward. Diamonds of common rounded dodecahedral morphology, for example, can be expected to approximate the shape of a convergent lens so that incident radiation will be focused through the sample and measured diamond thickness will underestimate the actual path length. To overcome this problem it would normally be necessary to resort to special sample polishing procedures. This route, however, was unavailable for most of the diamond specimens on loan to us, and an alternative method of determining optical path length, based on the strength of the two-phonon diamond lattice band at 2030 cm^{-1}, was devised. Since this band arises from vibrations of the carbon array, its strength will be proportional to the path length of IR radiation and will be independent of N concentration (Kaiser and Bond, 1959). We have measured the strength of the band at 2030 cm^{-1} for a number of optically flat diamond specimens, obtaining an absorbance of 0.47 ± 0.01 units per mm path length. This value yields an absorption coefficient of 10.8 cm^{-1}, slightly less than previously reported values of about 12 cm^{-1} for the band at 2030 cm^{-1} (e.g., Smith and Taylor, 1962). However, this value is dependent on the chosen base line, and for our specimens, reproducibility is increased by taking a linear base line between ~2700 cm^{-1} and ~1500 cm^{-1} for the path-length measurement (this accounts for the lower absorption coefficient). Thus for any nonplanar stone the strength of the band at 2030 cm^{-1}, when corrected for nonzero base line as above, may be divided by an absorbance of 0.47 mm^{-1} to obtain an actual path length.

In Figure 1 the path length (as determined above) has been plotted vs. measured thickness (using a micrometer) for the diamonds of this study. There is generally a 1:1 correspondence between measured thickness and path length for nonplanar diamonds of less than about 1.5 mm

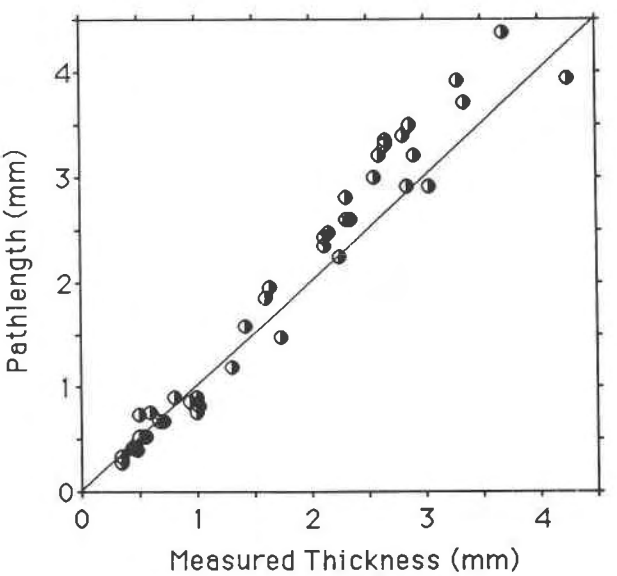

Fig. 1. Plot of optical path length determined from strength of the lattice band at 2030 cm^{-1} vs. measured diamond thickness for nonplanar diamonds analyzed in this work. Note departure of path length and thickness due to refraction in the larger diamonds.

thickness, indicating that refraction effects are only minor in these smaller stones. For thicknesses >1.5 mm there is a distinct departure from 1:1 behavior, showing that measurement of thickness significantly underestimates the actual path length as discussed above.

The above technique is limited to N contents of diamond of less than approximately 500 atomic ppm for >1 mm thicknesses because of saturation of the N defect bands (i.e., transmittance <1%) at higher N contents. This problem was encountered with about a third of the Copeton stones under investigation; some of these diamonds (CO17, CO20, CO21, and CO39) were broken to extract solid inclusions, and the spectra were then remeasured on smaller fragments (Table 1). A number of the higher N diamonds had intense platelet absorptions that saturated the IR detector even when smaller fragments were used; for these cases platelet intensities are designated "off-scale" in Table 1.

Some of the Argyle diamonds initially investigated (three eclogitic diamonds: A4, A44, A84, and one peridotitic diamond, A152, all documented by Jaques et al., 1989) had absorptions due to N defects that were very weak and could not be clearly distinguished from background noise; they were therefore not suitable for spectral decomposition. Because of their very low N contents (<10 atomic ppm) these diamonds may be type II specimens and have not been further considered in this work.

In a number of the larger diamonds, in particular, the N contents and proportions of A and B defects were found to be heterogeneously distributed from core to rim (cf. Milledge et al., 1989). This is consistent with a discontinuous growth history (Swart et al., 1983), as is particularly evident in coated diamonds (Boyd et al., 1987), or may reflect growth in an environment where there were fluctuations in f_{N_2} (e.g., Meyer, 1985). For the purpose of this paper, we where possible have chosen only core spectra and have not investigated intradiamond differences in N content or A/B ratio in any detail (this will form the subject of a future investigation). In Table 1 the extent of heterogeneity that can be expected using spectra recorded on different areas of specimens AA17, E4/7, and CO21 is documented.

Spectral decomposition

Spectral decompositions into A, B, and D defect components were carried out by a method modified after Clark and Davey (1984a) and Woods (1986) and separately from the path-length determination. First, the tail of the two-phonon diamond lattice absorption was subtracted using a synthesized spectrum with only two-phonon absorption features free of the N-induced defect bands. The synthesized spectrum was generated for each sample, using Digilab software, by fitting a smooth background to the region ~1600–500 cm^{-1} of the sample spectrum. Subtraction of the synthesized background from the original spectrum simultaneously normalizes the base line to essentially zero absorbance and removes the two-phonon tail. Nonzero base lines in the diamond spectra arise principally from surface reflectance, an effect that is fortunately not appreciably wavelength dependent, and base line variation in our data set was found to be essentially uniform with wavenumber over the region of interest. The spectrum was then scaled to a diamond thickness of 1 cm. Other minor absorptions, occurring mainly below 1000 cm^{-1} and designated G, H, and I by Clark and Davey (1984b), were not considered in the spectral decomposition. The N3 center, which absorbs in the visible spectrum and may be responsible for the pale yellow color of some of the Copeton diamonds, is typically present at low concentrations in diamond (<0.1–1% according to Woods, 1986) and has similarly not been considered in the spectra decomposition procedure.

Pure A, B, and D defect spectra over the range 1500–900 cm^{-1} were synthesized using Digilab software by addition of a series of Gaussian curves to duplicate the digitized spectra given by Woods (1986, Table A1). The pure spectra were then scaled to a N content of 1000 atomic

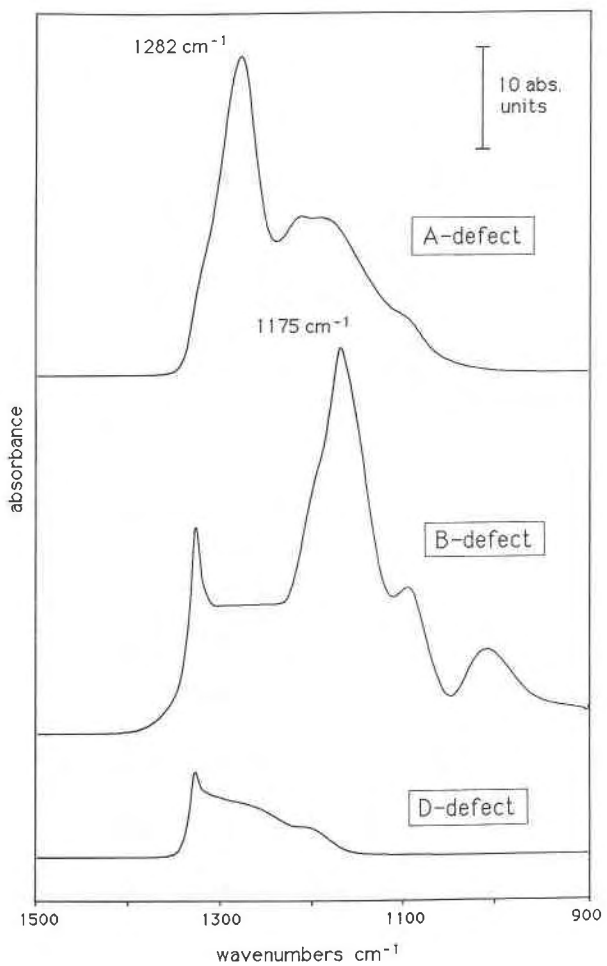

Fig. 2. Synthesized A-, B-, and D-defect IR spectra for a N content of 1000 atomic ppm and 1-cm diamond thickness.

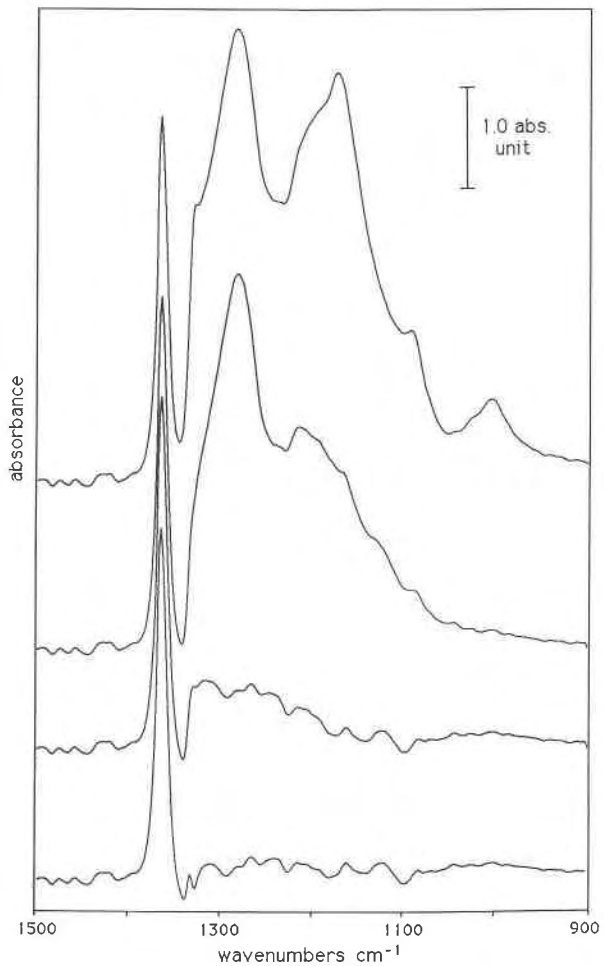

Fig. 3. Example of the spectral decomposition procedure for diamond DA131. Top spectrum is the FTIR absorption spectrum (scaled and corrected to base line) over the range 1500–900 cm^{-1} (A + B + D defects); middle spectra show results after subtraction of B-defect (leaving A + D) and A-defect components (leaving D only), respectively, and bottom spectrum is the residual after subtraction of the D-defect component. The sharp band at 1370 cm^{-1} (not subtracted) is the B′ absorption due to platelets.

ppm (i.e., 0.1 at.%) using the absorption coefficients at 1282 cm^{-1} given by Clark and Davey (1984a). The spectra are illustrated in Figure 2.

Spectral decompositions were carried out with the Digilab IMX software package. The pure spectra were sequentially subtracted from the sample spectra in the order A, B, D to achieve a zero absorbance base line in the region 1350–900 cm^{-1}. For samples with <90% A defects a second subtraction was performed in the order B, A, D. There was excellent agreement between the two subtractions, and the average value is quoted in Table 1. It was found that diamonds rich in A component did not contain any significant D defect content. An example of the spectral decomposition for diamond DA131 is illustrated in Figure 3.

In Table 1, the absorbances per cm thickness of diamond at 1282 cm^{-1} due to A, B, and D defects (represented by symbols μA, μB, and μD, respectively) are given. Total IR active N contents ($N_{tot}/10^{-3}$·atomic ppm) were calculated from Equation 3 of Clark and Davey (1984a): $N_{tot} = N_A + N_B + N_D = \mu A/300 + \mu B/120 + \mu D/50$. The constants in the equations are absorption coefficients (symbol α) determined at 1282 cm^{-1}. It should be noted that the B-defect absorption coefficient (αB) determined by Clark and Davey (1984a) is 50% higher than the earlier value reported by Evans and Qi (1982). This arises at least in part because Evans and Qi did not consider D defects in their spectral decomposition. The estimated uncertainties in the absorption coefficients are ±7% for αA and probably ±10–15% for αB and αD (Evans and Qi, 1982; Clark and Davey, 1984a). The percentage of total N occurring as A defects is given by $100 \cdot N_A/N_{tot}$ (listed in the fifth column in Table 1) and the total absorbance per cm thickness of diamond at 1282 cm^{-1} (i.e., $\mu A + \mu B + \mu D$) is given by μT (see Table 1).

The reproducibility of the spectral acquisition and decomposition procedure was tested by duplicate measurements on the same areas in several samples. It was found that the proportion of A defects (N_A) was reproducible to within ±4% relative and N content (N_{tot}) to within ±6% relative; these errors are significantly lower than the effects of sample heterogeneity and lead to only small uncertainties (<±2 °C) in the calculated N aggregation temperatures (see later). There is rather more uncertainty (~±20% relative) associated with the proportion of D-defect component (N_D) because of its generally low abundance, particularly in A-defect-rich samples. However, it should be pointed out that determination of the D-defect proportion is essential in recognizing a coherent N aggregation trend in a diamond population, particularly if B-defect-rich diamonds are present (Clark and Davey, 1984a). In earlier studies, where D defects have not been determined, A/B ratio can only give a qualitative guide to N aggregation state and regularities in the aggregation path may be obscured.

We found that the effect of uncertainties in the absorption coefficients (at the levels quoted above) do not lead to significant differences in the relative proportions of either A and B defects or total N contents among the diamonds studied, although the absolute values will differ. Interpretations made on the basis of the Clark and Davey (1984a) absorption coefficients should therefore be valid within the error limits specified. Even outside these bounds, the effect of an αB value some 20–30% lower on total N content is only significant for the B-defect-rich, high-N diamonds that make up a small proportion of our data set.

For each spectrum the platelet (or B′) peak was integrated over the range 1390–1348 cm^{-1} to give an integrated intensity represented by the symbol I(B′) in Table 1 (note that our units differ by a factor of ten from those used by Woods, 1986). The high frequency region of the spectrum was examined for the presence of the H-defect

band at 3107 cm^{-1} (Runciman and Carter, 1971; Woods and Collins, 1983) which, if present, was usually accompanied by a weaker band at 1406 cm^{-1}.

Results

Relationship between platelet peak strength and absorptions due to A, B, and D defects

Brozel et al. (1978) noted regularities in plots of IR absorption due to platelets as a function of the relative amount of A defects. This was extended by Woods (1986), who showed that a linear (inverse) relationship between platelet intensity divided by total absorbance [$I(B')/\mu T$] and the proportion of total absorption at 1282 cm^{-1} due to A defects ($\mu A/\mu T$) exists in a majority of type Ia diamonds (i.e., the regular diamonds). A minority of diamonds, exhibiting platelet degradation, plotted below this linear trend and mostly had $\mu A/\mu T < 0.4$. Woods (1986) also demonstrated that in diamonds containing only A defects, no platelet peak occurs. In Figures 4–6 we show graphically the relationship between $I(B')$ and the absorbance of A-, B-, and D defects for our data set.

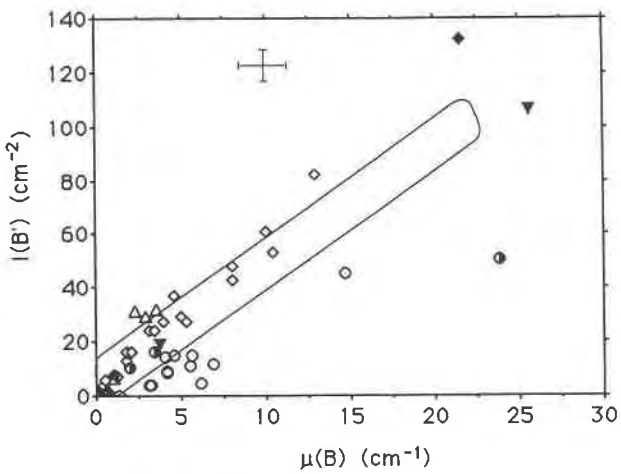

Fig. 5. Plot of platelet intensity vs. strength of the B-defect absorption. Symbols as given in Figure 4. Box outlines field of regular diamonds from Woods (1986). The plot generally mirrors Figure 4 but allows effective discrimination of Copeton and Ellendale-4 diamonds from Argyle diamonds.

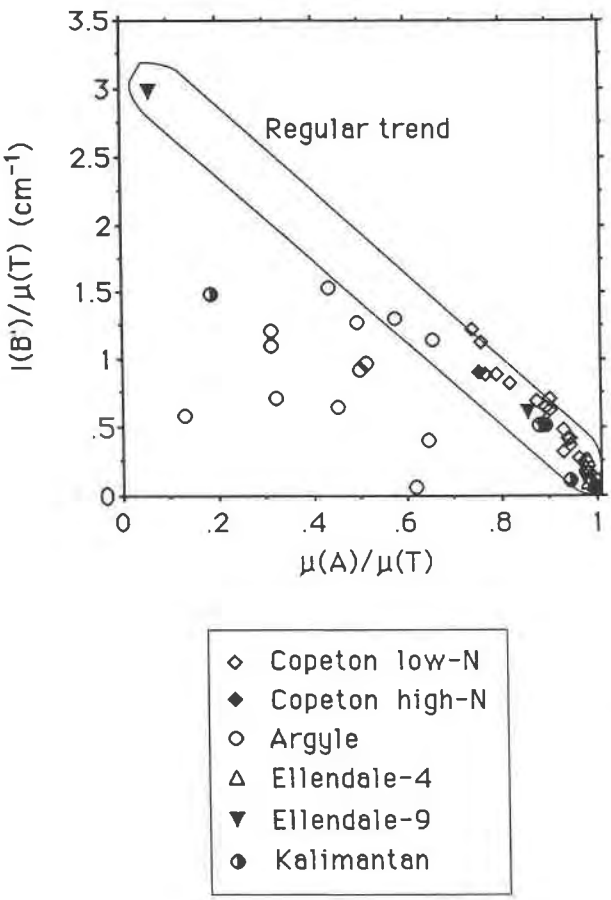

Fig. 4. Plot of platelet intensity vs. strength of A-defect absorption divided by total absorption, showing separation of diamonds into regular and irregular (i.e., platelet-degraded) groups. The Argyle eclogitic diamond population contains a high proportion of platelet-degraded stones.

Figure 4 shows a plot of $I(B')/\mu T$ (platelet intensity divided by total absorbance) vs. $\mu A/\mu T$(proportion of total absorbance due to A defects). The Ellendale diamonds, three Kalimantan diamonds, two Argyle diamonds, and most of the Copeton diamonds plot within the linear regular trend of Woods (1986). The majority of Argyle diamonds show much lower platelet peak intensities than would be expected from their $\mu A/\mu T$ values, and they clearly fall into the irregular group of Woods.

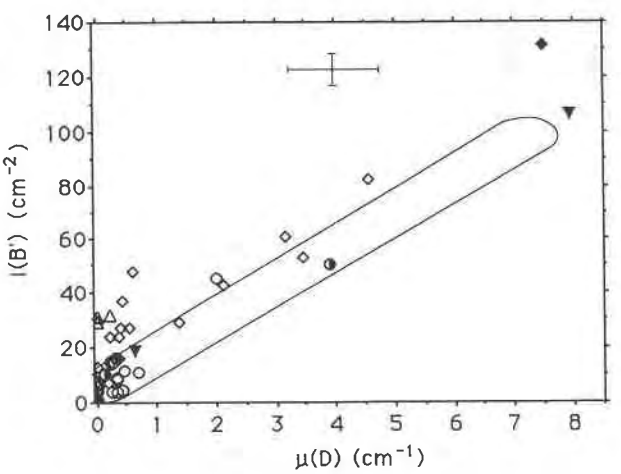

Fig. 6. Plot of platelet intensity vs. strength of the D-defect absorption. Symbols as given in Figure 4. There appear to be two groups: one group corresponding to the regular trend of Woods (1986) and another steeper trend comprising platelet-enriched or D-defect-poor diamonds, mostly from Copeton.

This is consistent with the spectroscopic work of Harris and Collins (1985), who showed that Argyle irregulars can have $\mu A/\mu T$ values as high as 0.88. One diamond from Kalimantan, KAL4, also falls within the irregular group.

Although the Copeton diamonds have a distribution shown in Figure 4 that generally conforms to regular behavior within experimental error, they tend to have slightly higher platelet intensities than would be predicted from their $\mu A/\mu T$ values and therefore plot above and to the right of the trend defined by the other regular diamonds. The A-defect-rich Copeton and Ellendale eclogitic diamonds have low to negligible platelet intensities, consistent with the observations of Woods (1986).

The trends seen in Figure 4 are also evident in a plot of platelet intensity [I(B′)] vs. absorbance at 1282 cm^{-1} due to B defects (μB) (Fig. 5). In agreement with the findings of Woods (1986), the Argyle diamonds and the Kalimantan irregular plot below the linearly correlated field of regular diamonds. Some of the Copeton diamonds and the Ellendale-4 diamonds plot slightly above this trend, whereas the Ellendale-9 peridotitic diamonds lie on the regular trend. The diagram is effective in discriminating between eclogitic diamonds from Argyle and those from Ellendale-4 and the dominantly eclogitic Copeton diamonds.

In a plot of I(B′) vs. μD, Woods (1986) showed that both regular and irregular diamonds formed a strict linear trend. A similar plot by Clark and Davey (1984a) showed more scatter, but a positive correlation was evident. In our data, plotted in Figure 6, a linear trend corresponding to that found by Woods (1986) is similarly identified. However, a significant portion of the low B-defect diamonds have higher I(B′) intensities than expected from their μD intensity and plot as a group above this trend. In diamonds of low B-defect content the error in determining the proportion of D defects is large so that at least some of the diamonds of the high I(B′) group may reflect this uncertainty.

The kinetics of A-defect aggregation

In order to obtain geologically useful information from the A → B aggregation reaction the kinetics of the reaction must be well understood. Evans and Harris (1989) modeled the A → B conversion on the assumption that the reaction follows second order kinetics (i.e., the rate-determining step involves the combination of two A defects). This assumption seems a reasonable one in view of recent models for the formation of the four N-atom B-defect by bulk diffusion and interaction of two A defects in the diamond lattice (Bursill, 1983; Bursill and Glaisher, 1985; Woods, 1986).

The second order rate law can be expressed by the equation $-d[A]/dt = k_2[A]^2$, where $[A]$ = concentration of A defects, t = time (s), and k_2 = second-order rate constant. This expression may be integrated over time and rearranged to give an equation for the concentration of A defects as a function of the total N content: $[A]_t = [A]_0/(1 + k_2 t[A]_0)$, where $[A]_t$ = A-defect concentration at time t and $[A]_0$ = initial A-defect concentration. From chemical reaction theory it can be assumed that the rate constant k_2 will follow an exponential dependency on temperature by an Arrhenius relationship: $k_2 = A \exp(-E_a/RT)$, where A = Arrhenius constant, proportional to the frequency at which two A defects encounter each other during random diffusion through the diamond structure, and E_a = activation energy for A → B conversion.

Calibration of the kinetic equations

From the above equations it is apparent that the extent of A → B conversion will depend on the temperature history of diamond while it was resident at high temperatures in the mantle (the k_2t term) and its initial N concentration ($[A]_0$). The constants in the kinetic equations may be determined either from high pressure and high temperature experiments or from natural diamonds. In the latter case, in addition to measurement of the diamond's N aggregation state, independent knowledge of the diamond's age, age of emplacement of the kimberlite or lamproite that brought the diamond to the Earth's surface, and the temperature prevailing during mantle residency is required. The mantle storage temperature may not necessarily be the same as the temperature of diamond formation; for example, a decrease in the geothermal gradient will result in storage temperatures that are lower than those of diamond formation (see below). Evans and Harris (1989) determined a value of E_a from two Finsch diamonds using a model age of 3.3 Ga (Richardson et al., 1984) and an average storage temperature estimated from olivine-garnet thermometry. A value for the Arrhenius constant, A, was taken from the high temperature and high pressure experimental data of Evans and Qi (1982).

The availability of further experimental data on diamond (Clark and Davey, 1984a) and information from mineral inclusions in the Argyle eclogitic diamonds giving crystallization age (Richardson, 1986) and equilibration temperature data (Jaques et al., 1989) has prompted us to attempt refinement of the values of both E_a and A. Our approach is to determine E_a and A from an Arrhenius plot (a plot of ln k_2 vs. $1/T$) so that all the experimental and natural data can be simultaneously regressed. Such a plot should be linear with a slope of E_a/R and an intercept of ln(A) if an Arrhenius relationship is valid.

Several uncertainties are introduced in attempting to use natural diamond data to calibrate the kinetic equations. The first involves the assumption that all diamonds of one paragenesis from a particular pipe formed at the age given by the dating of a suite of inclusions in diamonds of that paragenesis. The good agreement between ages obtained from ^{40}Ar-^{39}Ar laser-probe dating of pyroxene inclusions from Premier eclogitic diamonds (Phillips et al., 1989) with that obtained by Sm-Nd isochron dating for garnet and pyroxene composites (Richardson, 1986) suggests that this assumption may be approximated by at

least certain diamond populations. On the other hand, the wide range in Sm-Nd model ages reported by Smith et al. (1989) for eclogitic garnets from the Finsch pipe implies that this may not be generally true, and even within a single locality diamonds of similar paragenesis might have formed at different times.

Uncertainties are also introduced in assuming that temperatures prevailing during a diamond's residence in the mantle may be equated with crystallization temperatures obtained by silicate geothermometry from isolated mineral inclusions (i.e., nontouching silicates dispersed within diamond). If ambient mantle temperatures (=diamond storage temperatures) rose or fell after diamond formation (and incorporation of the inclusions) then the N aggregation process would be accelerated or retarded, respectively. This change in temperature would not be recorded by isolated (nontouching) silicate inclusions; only adjacent, contacting (touching) grains would reequilibrate. The assumption that crystallization temperature equates with mantle storage temperature would result in either the overestimation or underestimation of the value of E_a. The fact that studies have shown that temperatures obtained from isolated olivine-garnet inclusion pairs in diamond are higher than those obtained from chemically equivalent mineral pairs from the same pipe suggests that cooling and reequilibration of the mantle does take place after diamond formation in some terranes (Pohkilenko and Sobolev, 1986).

An additional uncertainty is introduced by heterogeneity in the N aggregation state of the diamond. Multiple periods of growth (and resorption) of diamond are indicated by internal growth zoning (e.g., Seal, 1965) and by zoning in C and N isotopic compositions in diamond (e.g., Swart et al., 1983; Boyd et al., 1987). Griffin et al. (1988) inferred from a study of trace element contents in diamond inclusions that diamonds grew in an open system, possibly over a period of time. Extrapolations and uncertainties are therefore inherent in linking the N aggregation state determined by IR measurements on a single diamond (or even part of a single diamond) to diamond formation ages and ambient mantle temperatures inferred from crystallization temperatures of mineral inclusions.

Nonetheless, errors introduced by the above uncertainties can be minimized by careful selection of diamonds, and we have adopted the following criteria in selecting natural diamonds to include in the Arrhenius plot: (1) Silicate geothermometry must give similar temperatures for nontouching inclusions in diamond and touching inclusions or geochemically equivalent xenoliths (reflecting constancy of temperature during the period of mantle residency). (2) The diamonds must have a well-constrained and preferably short mantle residence time (t_{MR}) to minimize the effects of any cooling or heating following diamond formation. (3) The diamonds ideally should have resided in the mantle for at least 50 Ma at relatively high temperatures, preferably >1200 °C, to minimize the effects of significant changes in mantle residence temperature (essentially cooling) on the progression of N aggregation, since, as will be shown later, any cooling history has less effect on diamonds with low A/B defect ratios.

Conditions 1 and 2 are met by the Finsch diamond F13 and xenoliths XM48 (Shee et al., 1982) and HRV247 used by Evans and Harris (1989). However, diamond F39 has an inclusion temperature 130 °C lower than the average xenolith temperature of ≈1100 °C (Shee et al., 1982; Kesson and Ringwood, 1989). Evans and Harris (1989) attempted to overcome this problem by simply assigning a single average temperature of 1130 °C to samples F39, F13, and XM48. This choice is, however, somewhat arbitrary and, in view of the small number of data points, we have chosen instead to regress the actual temperatures determined from silicate geothermometry and to exclude diamond F39 from the regression.

Eclogitic diamonds from Argyle (Jaques et al., 1989) have an average inclusion temperature (both touching and nontouching) of ≈1255 °C (for P = 5.0 GPa) and a short mantle residency (400 Ma: Richardson, 1986) and therefore meet the criteria 1 to 3. Because individual inclusion data are not available for each of the ten Argyle diamonds studied (Table 1), for the purposes of the Arrhenius plot we have assigned an average temperature of 1255 °C from Jaques et al. (1989). This is justified since the ln k_2 values span a narrow range and the number of samples is sufficiently large so that the mean temperature has some statistical significance.

High temperature experimental data on A → B conversion at 2400–2700 °C under pressure was obtained from the studies of Evans and Qi (1982) (three data points from two natural diamonds) and Clark and Davey (1984a) (diamonds: A4, D4, A1, and A2). The uncertainty in experimental temperature was not quoted but for a multiple-anvil high-pressure apparatus of the type used in these studies it is estimated to be ±100 °C (Holloway and Wood, 1988).

Figure 7 shows the Arrhenius plot using the above data. Linear regression gives E_a/R = 81626 ± 1290 K and ln(A/atomic ppm^{-1} s^{-1}) = 13.507 with a regression coefficient (r) of 0.998. The temperature dependence of the A → B aggregation reaction clearly conforms to Arrhenius-type behavior. The value of E_a in eV units is 7.03, which compares favorably with the mean value of 6.88 eV determined by Evans and Harris (1989). The lower value of 6.5 eV suggested by Kesson and Ringwood (1989) is not consistent with our data.

It has been suggested (Bursill and Glaisher, 1985; Woods, 1986; Milledge et al., 1989) that diamonds such as Argyle, which show platelet degradation, may also lose N to IR inactive sites. Underestimation of total N content, as determined from IR measurements, would result in higher estimated aggregation temperatures. Therefore, if N had been lost to IR inactive sites in any significant amount, the Argyle diamonds should record higher temperatures than expected from the Arrhenius regression. Inspection of Figure 7 suggests that this is not the case. In fact, exclusion of the Argyle diamond data from the

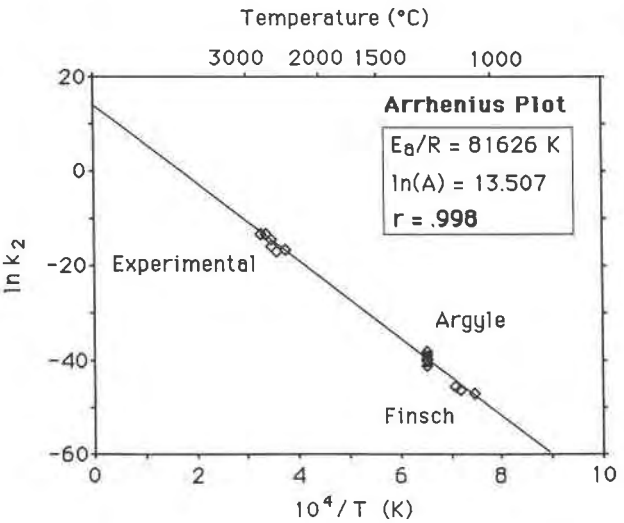

Fig. 7. Arrhenius plot for the second-order A → B aggregation reaction using experimental and natural data (Argyle and Finsch diamonds). Note the strong linear correlation. The activation energy for the conversion is 7.03 eV, close to the estimate of Evans and Harris (1989).

regression gives a value for E_a only marginally higher (7.15 eV vs. 7.03 eV), resulting in an average calculated temperature only 14 °C higher than is the case for E_a = 7.03 eV. This is well within reasonable uncertainties associated with the geothermometric and age data and implies no significant loss in IR active N from A, B, and D defect sites in Argyle diamonds.

Relationships among temperature, mantle residency time (t_{MR}), and N content of diamond

The kinetic equations may be used to model the relationships among the relative proportions of A defects, storage temperature, time, and N content of diamond. In Figures 8A–8C we have considered diamond with a range of N contents from 0–1250 atomic ppm resident in the upper mantle for periods (symbol t_{MR}) of 3.2 Ga, 1.6 Ga, and 0.4 Ga. The residency period of 3.2 Ga is the same as that determined for Finsch peridotitic diamonds (Richardson et al., 1984) and a residency of 0.4 Ga has been determined for Argyle eclogitic diamonds (Richardson, 1986). Plotted on the figures are a series of isotherms depicting the extent of A → B conversion as a function of total N concentration. As expected from the kinetic equations, the extent of conversion at a given temperature increases with increasing N concentration. For example, for mantle storage temperatures of 1100 °C a diamond with ~1000 ppm N will have undergone conversion of almost 50% A defects to B defects after 3.2 Ga. Conversely, at the same temperature a diamond with ~200 ppm N would only have about 10% B defects after 3.2 Ga. The plots show that for long storage times for diamond in the upper mantle, the extent of N defect aggregation will be sensitive to temperatures in the range 1050–1300 °C, which agrees with the results of Evans and

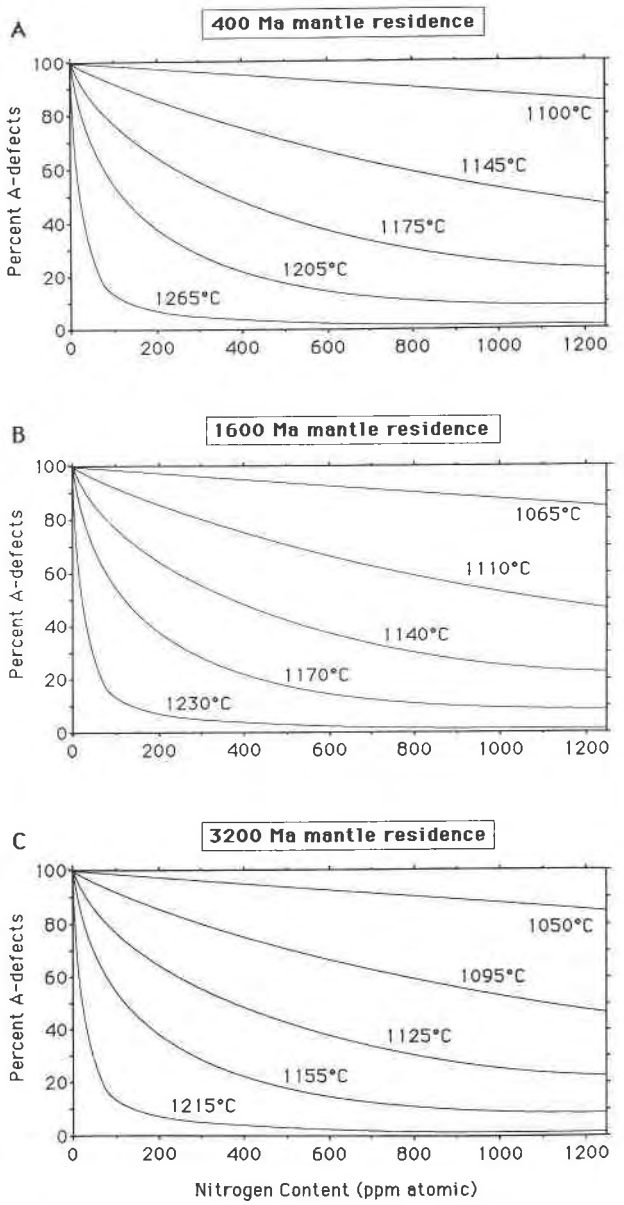

Fig. 8. Results of kinetic modeling of the A → B aggregation reaction displayed as a series of isotherms in plots of % A defects vs. N content for mantle residence times of 400 Ma (**A**), 1600 Ma (**B**), and 3200 Ma (**C**). To achieve similar A → B conversions to t_{MR} = 3200 Ma, diamond storage temperatures must be 15 °C higher for t_{MR} = 1600 Ma and 50 °C higher for t_{MR} = 400 Ma.

Harris (1989). At temperatures < 1050 °C there is no significant conversion of A defects, even for diamond formation in Archean times, whereas at temperatures > 1300 °C conversion is near completion after only a few hundred million years. Note that there would be no significant effect on N aggregation state resulting from entrapment and transport of diamond in a hot kimberlite or lamproite melt on the short time scales (~hours, days, e.g., Spera, 1984) required to transport these magmas and

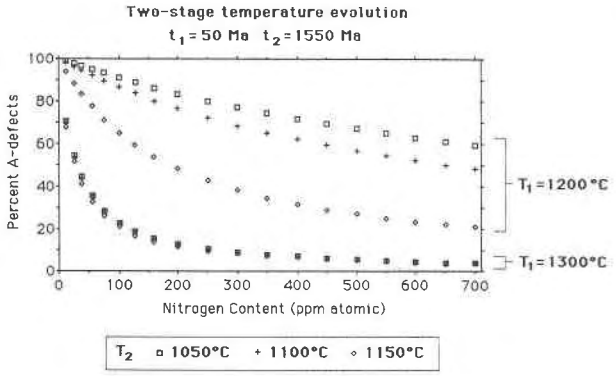

Fig. 9. An illustration of the effects of falling geothermal gradient (two-stage temperature evolution model) on the extent of A → B aggregation. The curves show the effect of 50 Ma (t_1) storage at T_1 (either 1200 °C—upper curves—or 1300 °C—lower curves) followed by cooling, then 1550 Ma (t_2) storage at 1150 °C, 1100 °C, or 1050 °C (T_2). The effects of cooling on the extent of N aggregation are less for diamonds that have been stored at high temperatures for some time during their evolution. Temperatures recorded by N aggregation (T_{NA}) will be average values reflecting heating or cooling of the lithospheric mantle since diamond formation.

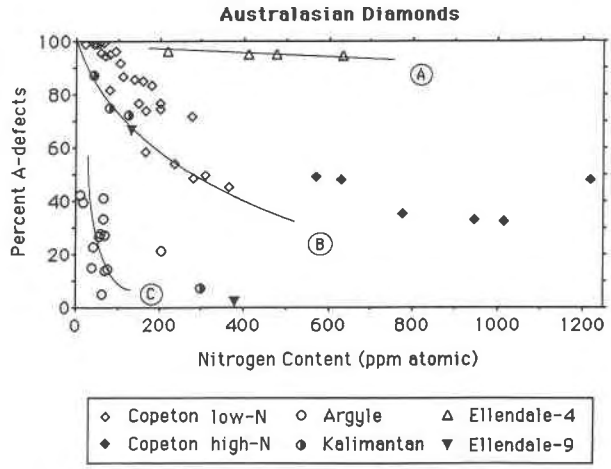

Fig. 10. N aggregation plot analogous to Figure 8 for the Australasian diamonds investigated in this study. Ellendale-4 eclogitic diamonds plot on a low temperature isotherm (A) in contrast to Argyle eclogitic diamonds which cluster about a high-temperature isotherm (C). The majority of Copeton diamonds, including low-N and high-N groups, plot on a series of moderate temperature isotherms. A remarkable feature of the diagram is the coincidence of diamonds from Ellendale-9, central and west Kalimantan and Copeton on an isotherm at 1145 °C (B). This similarity in thermal history suggests these diamonds may have had a common origin in ancient Gondwanaland subcontinental lithosphere (see text).

their xenocrysts from mantle depths. With increasing temperature the shape of the isotherms changes from linear to logarithmic, reflecting the dominance of the Arrhenius term at higher temperatures.

To achieve A → B conversions comparable to those for t_{MR} = 3.2 Ga, storage temperatures for diamonds resident in the mantle for only 1.6 Ga (t_{MR} = 1.6 Ga) must be 15 °C higher than those where t_{MR} = 3.2 Ga. For an even shorter mantle residence time, t_{MR} = 0.4 Ga, temperatures must be 50 °C higher. Since most silicate geothermometers are accurate to only ±30–50 °C, it is evident that the kinetic equations cannot, as yet, be used to provide a very accurate estimate of diamond age. However, it should be possible to distinguish between an ancient diamond population with t_{MR} ~1–3 Ga (i.e., a Proterozoic to Archean age) and a much younger diamond population with t_{MR} ~0.01–0.3 Ga (i.e., a Phanerozoic age). It should be noted that diamond age = t_{MR} + age of kimberlite or lamproite host.

In the above discussion we have assumed that storage temperatures remained constant during the diamond's residence period in the mantle. If this is not the case then the storage temperature determined from the N-defect aggregation state (which we have designated T_{NA}) will be an average value reflecting rising or falling geothermal gradients in the mantle. T_{NA} may therefore not necessarily correspond to temperatures determined from diamond inclusions that record the formation temperature (non-touching types) or the last metamorphic reequilibration temperature affecting diamond (touching inclusions). This behavior is illustrated in Figure 9, which shows the effect on N aggregation of two stages of temperature evolution. The first stage is 50-Ma evolution at either 1200 °C or 1300 °C, followed by cooling and a further 1550-Ma evolution at temperatures of 1050, 1100, and 1150 °C. For the 1200 °C initial temperature, final T_{NA} values are 1115, 1123, and 1157 °C, which compares with the time-weighted average temperatures of 1055, 1103, and 1152 °C, respectively. For the 1300 °C initial temperature, final T_{NA} values are all close to 1210 °C; the corresponding weighted averages are 1059, 1106, and 1155 °C.

It is evident from the above data that the final T_{NA} values do not, in general, correspond to a simple time-weighted mean temperature but are affected more by the higher temperature evolution stage. However, provided mantle storage temperatures do not differ by more than about 50 °C from diamond formation temperatures, then T_{NA} will be close to the time-weighted mean and can thus serve as a geothermometer. As shown by the lower curve in Figure 9, if T_{NA} exceeds about 1200 °C, then such values will not record any significant cooling history. An important point is that T_{NA} values alone cannot yield information on the magnitude or duration of changes in ambient mantle temperatures. Additional data from silicate inclusion and xenolith geothermometry can provide useful constraints on such changes however.

Application of the kinetic equations to Argyle, Ellendale, Kalimantan, and Copeton diamonds

In Figure 10 are plotted the percentage of A defects vs. total N content (N_{tot}) for the Argyle, Ellendale, Kalimantan, and Copeton diamonds. For graphical purposes the

Copeton diamonds have been divided into a high N group (>500 ppm N with mostly pale yellow colors) and a low N group (<400 ppm N and mostly colorless). As will become apparent from the results given below, many of the diamonds have N aggregation temperatures that conform closely to the isotherms predicted by the kinetic equations as illustrated in Figure 8. The assumption of second-order kinetics for the A → B aggregation reaction therefore appears to be a valid one.

Ellendale-4 eclogitic diamonds. The Ellendale-4 eclogitic diamonds comprise a suite of A-defect dominant diamonds that show little variation in the extent of conversion of A defects with N concentration and define a linear low-temperature isotherm in Figure 10 (cf. Fig. 8). If these diamonds are Proterozoic in age and formed at about the same time as the Argyle eclogitic diamonds (so that t_{MR} = 1.6 Ga using a Miocene age for the Ellendale lamproites) then they evolved in cool lithosphere with T_{NA} = 1066 ± 7(1σ) °C. If they are younger than 1.6 Ga, for example, 0.4 Ga, then T_{NA} would be 1100 °C. These temperatures contrast with the much higher temperatures >1200 °C experienced by Argyle eclogitic diamonds.

Silicate inclusion geothermometry allows some constraints to be placed on the age of the Ellendale-4 diamonds. Two pieces of evidence suggest that they are much younger than Argyle diamonds. First, the average T_{NA} value of 1066 °C calculated for t_{MR} = 1.6 Ga lies on the graphite-diamond transition or just within the graphite stability field for typical shield geotherms (40–44 mWm^{-2}), indicating that a residence time of 1.6 Ga must represent the maximum possible value. Second, the garnet-clinopyroxene inclusion temperature of 1115 °C determined by Jaques et al. (1989) for an Ellendale-4 eclogitic diamond gives a calculated residency time of ≈150 Ma, indicating a Mesozoic age. Provided this temperature is representative of the diamond population and no significant lithosphere cooling has occurred—and these appear to be reasonable assumptions since 1115 °C is close to the average temperature (1123 °C) recorded by Ellendale peridotitic diamonds (see later)—then a Phanerozoic age is the most likely for the Ellendale-4 eclogitic diamonds. At about 1115 °C an uncertainty of ±30 °C indicates a corresponding uncertainty bracket in t_{MR} of 500–50 Ma.

Copeton diamonds. At present there are no geothermometric or isotopic data available for the Copeton diamonds, and therefore detailed constraints on t_{MR} are not possible. We have assumed for comparative purposes that t_{MR} = 1.6 Ga; if t_{MR} is less than 1.6 Ga, as suggested by the absence of Precambrian crust in the Copeton region (Wyborn, 1989), the average mantle storage temperatures will be higher (see Fig. 8).

Both the high and low N Copeton diamonds are represented in Figure 10 by a series of moderate-temperature isotherms. The temperature distribution is shown in Figure 11. The isotherms appear to be essentially continuous across the two diamond groups, and no platelet-degraded diamonds are present. The highest temperature isotherm at T_{NA} = 1144 °C (for t_{MR} = 1.6 Ga) or 1179 °C (for t_{MR} = 0.4 Ga) is the best defined (see Fig. 10) and is constrained by six low-N diamonds [1σ standard deviation (sd) = 3 °C]. The temperature data suggest further isotherms at T_{NA} = 1132 °C (for t_{MR} = 1.6 Ga; defined by five points; 1σ sd = 2 °C), at T_{NA} = 1125 °C (for t_{MR} = 1.6 Ga; defined by five points; 1σ sd = 3 °C) and at T_{NA} = 1110 °C (for t_{MR} = 1.6 Ga; defined by eight points; 1σ sd = 5 °C). Six of the Copeton diamonds with <100 ppm N have T_{NA} values below 1100 °C. One of these (CO30) has negligible platelet intensity, indicating low temperature storage or short-term mantle residency.

In the high-N diamonds CO3 and CO39, coesite has been identified as an inclusion, indicating that these belong to the eclogitic paragenesis. The smaller proportion of the diamonds that are peridotitic are therefore likely to be represented by a portion of the lower N colorless stones.

Kalimantan and Ellendale-9 peridotitic diamonds. Three of the Kalimantan alluvial diamonds (two from western Kalimantan and one from central Kalimantan) and one Ellendale peridotitic diamond (E9/9) lie on an isotherm at T_{NA} = 1145 °C (1σ sd = 4 °C) for t_{MR} = 1.6 Ga (or T_{NA} = 1180 °C for t_{MR} = 0.4 Ga), coincident with the highest temperature Copeton isotherm described above.

The other central Kalimantan diamond, KAL4, and Ellendale diamond, E9/16, have T_{NA} values (for t_{MR} = 1.6 Ga) of 1209 °C and 1241 °C, respectively, and have experienced much higher temperatures, consistent with an origin near the base of the lithosphere. KAL4 is also a platelet-degraded diamond, a characteristic of most Argyle eclogitic diamonds. However, other features such as absence of H defects and a higher N content indicate that it must have grown and evolved in a mantle environment that was distinct from that hosting the Argyle eclogitic suite.

Temperatures determined for four peridotite suite inclusions from Ellendale-4 peridotitic diamonds (none was available from Ellendale-9) using the recent pyroxene thermometer of Brey (1989) for P = 5.0 GPa give a range of values: 1096–1149 °C (mean 1123 ± 22°C). Two higher temperatures, 1175 and 1235 °C, were recorded for garnet-olivine and pyroxene pairs by Jaques et al. (1989). This range of temperatures is in broad agreement with the T_{NA} values of diamonds E9/9 and E9/16 if they formed during late Archean to mid-Proterozoic times.

Argyle eclogitic diamonds. Argyle eclogitic diamonds are characterized by low N contents (mostly <100 atomic ppm), high proportions of B defects, the presence of H defects, and platelet degradation. In Figure 10, the data points do not lie on a single isotherm but have a distribution about a mean value (1262 °C) as shown by the histogram in Figure 11. This compares with the distribution of garnet-clinopyroxene inclusion crystallization temperatures about a mean of 1247 °C determined by Jaques et al. (1989). The lower and higher diamond inclusion temperatures (<1200 °C and >1400 °C) recog-

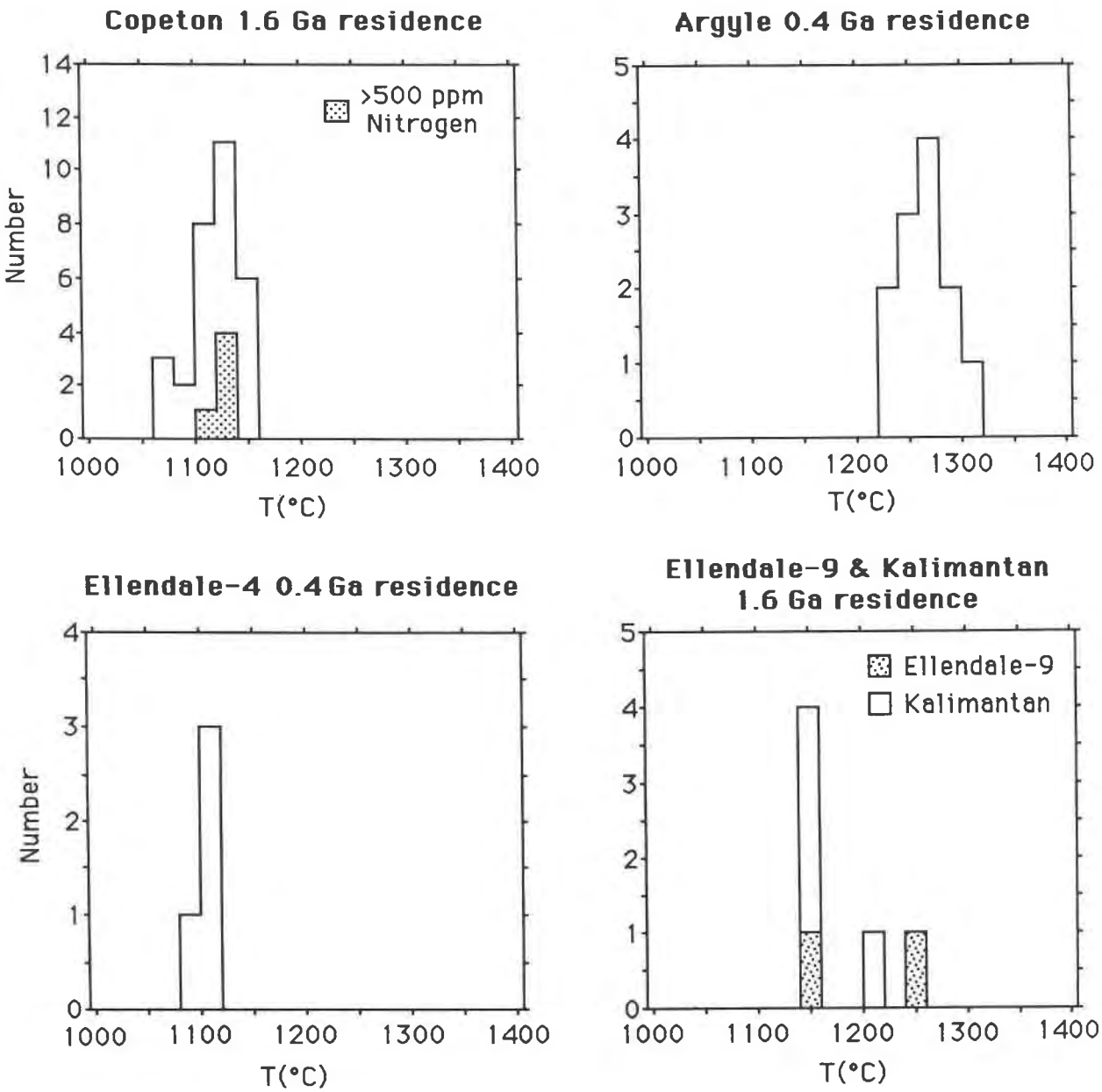

Fig. 11. Histograms showing the distribution of T_{NA} values for various mantle residency periods.

nized by Jaques et al. (1989) are not represented among our data set, possibly as a consequence of thermal re-equilibration of the diamonds during mantle storage. The two pale yellow stones (A201 and A204) record the lowest N aggregation temperatures, ≈1225 °C, and the possibility exists that they represent a time-temperature population distinct from the more common brown stones (i.e., formed in a lower *P-T* environment or at a slightly later time).

H defects

All the Argyle eclogitic diamonds studied show the presence of H defects identified by the absorption at 3107 cm^{-1}. Most of the Copeton high-N diamonds also contain H defects. In the other diamonds of the data set, H defects occur sporadically, and their occurrence does not clearly correlate with other parameters. The irregular diamond KAL4 does not contain H defects, indicating that platelet degradation and H-defect formation are probably not related processes.

Heterogeneity in N distribution

The extent that heterogeneities in N distribution affect T_{NA} has been investigated for diamonds CO21, AA17, and E4/7 (Table 1). For CO21 and E4/7, N content varies by ≈7% and ≈15%, respectively, in the two areas ex-

amined in each sample; the percentage of A defects, however, varies sympathetically, and T_{NA} differs only by 1 °C. Thus there is no evidence for a multistage growth history separated by long time intervals in these samples, and variations in N content are presumably due to N depletion in the diamond growth medium.

In diamond AA17, N content varies by about 20%, but the proportion of A defects does not vary sympathetically, resulting in a 14 °C spread in temperatures. This difference is sufficient to suggest a multistage growth history but one within the general growth environment of other Argyle diamonds (rather than a regime fundamentally distinct in P, T, f_{O_2}, and time, as is the case for the coats on certain diamonds: Chrenko et al., 1967; Haggerty, 1986; Boyd et al., 1987). This view is supported by the similarity in $\delta^{13}C$ values (varying from only -10.6 to -11.0‰) determined on different portions of AA17 (Jaques et al., 1989).

Discussion and conclusions

Nature of diamond source regions of the Kimberley Block

Figure 10 illustrates the distinct difference in the time-temperature characteristics of eclogitic and peridotitic diamonds from Argyle, Ellendale-4, and Ellendale-9. Of particular note is the contrast between the highly aggregated but N-poor Argyle eclogitic diamonds of the East Kimberley region and the poorly aggregated but N-rich Ellendale eclogitic diamonds of the West Kimberley region. Although they have very different N aggregation characteristics, both these diamond populations were resident in subcontinental lithosphere underlying the Proterozoic mobile belts that flank the eastern and southwestern margins of the Kimberley craton (Jaques et al., 1986). Xenolith studies have demonstrated that the lithosphere of this region has a thickness comparable to the lithospheric roots beneath Archean cratons (Jaques et al., 1990). This has led to the hypothesis that there may be little difference in lithospheric thickness between Archean cratons and cratonized early Proterozoic mobile belts; alternatively, the mobile belts are underlain by Archean lithosphere. Some constraints on these alternatives are provided by the N aggregation data.

Argyle eclogitic diamonds. The Argyle eclogitic diamonds are thought to have been resident near the base of the lithosphere following their formation approximately 200 Ma after cratonization of the Kimberley block at ~1.8 Ga (Jaques et al., 1989, 1990). During their 400 Ma residency period, prior to emplacement at the surface, an event (or events) took place that caused extensive platelet degradation. This event was probably also responsible for the predominance of plastic deformation textures among the Argyle diamonds. At present, the causes of platelet degradation are speculative, but high temperatures combined with shearing stress may be important factors in promoting degradation (Woods, 1986). If this is so, then the Argyle diamonds may have recorded a continental rifting or migration event reflecting proximity to upwelling asthenospheric mantle at the base of the lithosphere (cf. Haggerty, 1986).

The Arygle eclogitic diamonds are distinct from the small percentage of Argyle diamonds that carry peridotitic inclusions. These latter diamonds do not show the marked resorption and deformation features displayed by the eclogitic population and so have evidently not experienced a similar thermomechanical history, despite also having an origin near the base of the lithosphere (Jaques et al., 1990). If the Argyle eclogitic lithosphere resulted from accretion to basal peridotitic lithosphere (cf. Helmstaedt and Schulze, 1989) sometime between 1.6 and 1.2 Ga, then the platelet-degraded nature of the Argyle diamonds may reflect transport of diamondiferous eclogite through hot, convective asthenosphere from a source region remote from its eventual East Kimberley location.

Ellendale eclogitic and peridotitic diamonds. In contrast to the Argyle eclogitic diamonds, the Ellendale-4 eclogitic diamonds of the West Kimberley region do not record any platelet degradation events and have been resident in relatively cool, stable lithosphere. Geothermometry constraints dictate that they must be significantly younger than the Argyle diamonds. This suggests the diamondiferous eclogitic lithosphere of the East and West Kimberley regions have had separate origins in both space and time.

The N defect aggregation state of the two Ellendale-9 peridotitic diamonds studied is also consistent with prolonged stability of the West Kimberley subcontinental lithosphere. The regular, B-defect-rich diamond E9/16 has not experienced platelet degradation and has evidently had a long undisturbed mantle history at relatively high temperatures. This indicates probable storage near the base of the lithosphere from Archean to mid-Proterozoic times. Diamond E9/9 belongs to a separate population that is either younger than E9/16 or was resident in a cooler, interior portion of the lithosphere.

The role of subduction in the genesis of Kimberley diamonds. The above discussion emphasizes the range of diamond source regions in lithosphere underlying the mobile belts of the Kimberley block. We find that diamond formation is not restricted to one particular time interval but that conditions suitable for diamond formation have evidently existed throughout the history of the block. The stability of the West Kimberley lithosphere suggests that the western mobile belt (the King Leopold mobile belt) is underlain by Archean subcontinental lithosphere of the Kimberley craton, whereas the East Kimberley lithosphere (Halls Creek mobile belt) has been underplated by eclogite and may represent the boundary zone between two tectonic blocks (Jaques et al., 1990).

The mechanisms by which diamondiferous eclogites are incorporated into stable subcontinental lithosphere at times well after cratonization is an intriguing problem. The phenomenon is evidently common to other cratonic areas such as the Kaapvaal craton, where multiple Proterozoic eclogite formation events, in some cases essen-

tially synchronous with kimberlite magmatism, are recorded (e.g., Philips et al., 1989). Such observations are at least partly reconcilable with recent models that suggest eclogites represent former basaltic crust (in part modified by remelting) that has accreted onto the base of the lithosphere during shallow-angle subduction (Helmstaedt and Gurney, 1984; MacGregor and Manton, 1986; Helmstaedt and Schulze, 1989; Kesson and Ringwood, 1989).

In the case of East Kimberley lithosphere, we interpret the diamond formation event as occurring in a remote location (in subducted crust beneath a continental block adjacent to the Kimberley craton?), whereas for that of West Kimberley, diamond formation probably took place in situ at a time well after cratonization. It is difficult to envisage how subduction could be responsible for eclogite formation in proximity to old cratonic nuclei that have no record of postcratonization orogenic activity. Eclogitic diamond formation must therefore reflect the operation of additional processes.

One such process offering a plausible explanation for eclogitic diamond formation is the redox melting model discussed by Green et al. (1987) and Taylor and Green (1988, 1989). Diamond formation was interpreted to result from interaction between relatively oxidized mantle material (e.g., subducted basalt previously incorporated at the base of the lithosphere) and reduced mantle C-O-H fluids. Such fluids could cause remelting of eclogitic lithosphere and concentration of diamond or graphite in the melt residues, provided sufficient initial redox contrast exists between the fluid and rock (Taylor and Green, 1989). Subducted basalt ($f_{O_2} \geq$ FMQ) would be a suitable host for melting and diamond precipitation by interaction with CH_4 bearing reduced ($f_{O_2} <$ MW) mantle fluids. By this mechanism ancient eclogitic material stored at the base of the lithosphere can be enriched in diamond by localized fluid activity at any stage during the history of the craton. C enrichment may also take place within the slab during subduction (see Fig. 6 of Green et al., 1987).

It follows from this mechanism that the large range of $\delta^{13}C$ values ($\sim +3$ to -30‰), typical of eclogitic diamonds (Sobolev et al., 1979; Deines, 1980; Sobolev, 1984; Deines et al., 1989), can be accounted for by variable input of recycled crustal C from the original subducted basalts and input of mantle C ($\delta^{13}C \approx -5$‰) from the C-O-H fluid phase. Since Ellendale-4 eclogitic diamonds have a mean $\delta^{13}C$ value of -4.9‰ (Jaques et al., 1989), we predict minimal crustal C input in this case and hence diamond enrichment of originally C-poor eclogitic lithosphere. For Argyle diamonds, which have an average $\delta^{13}C \approx -11$‰, a recycled crustal carbon component is inferred (Jaques et al., 1989, 1990).

Although the number of samples for which we have both ^{13}C isotopic data and N data is small (isotopic data listed in Jaques et al., 1989), we find that on a plot of ^{13}C vs. N content diamonds from Argyle and Ellendale cluster into two separate groups. Ellendale diamonds show a negative $\delta^{13}C$-N_{tot} correlation with a large range of N contents reminiscent of the trend identified for a portion of the peridotitic diamonds from Finsch and Premier (Deines et al., 1989; Fig. 2), whereas Argyle diamonds show no $\delta^{13}C$-N_{tot} correlation and have low N and ^{13}C contents. Deines et al. (1989) have suggested that low N diamonds may be characteristic of high temperature and low f_{O_2} formation environments, and this is in agreement with the conditions determined for the Argyle diamond source region (Jaques et al., 1989, 1990). It is not clear what processes cause the negative $\delta^{13}C$-N_{tot} correlation observed for Ellendale and some South African diamonds.

A common diamond source region in subcontinental mantle of northeastern Gondwanaland?

A remarkable feature of Figure 10 is the coincidence of diamonds from western Kalimantan (two stones), central Kalimantan (one stone), Ellendale-9 (one stone), and Copeton (six stones) on a single time-temperature isotherm corresponding to 1145 °C for $t_{MR} = 1.6$ Ga (or 1180 °C for $t_{MR} = 0.4$ Ga). To achieve such a tightly constrained isotherm, we propose that these diamonds have had similar mantle residence times and have experienced very similar thermal histories. If the diamonds originated in unrelated subcontinental lithosphere, it would seem remarkable that such coincidence could be achieved in view of the very different tectonic, thermal, and magmatic histories expected for separate lithospheric blocks. Therefore, the distinct possibility exists that these diamonds originated in a common ancient subcontinental lithospheric source region now geographically dispersed by more recent tectonic processes. It follows from this argument that, since Ellendale diamonds were erupted at the surface during the Miocene, the alluvial Kalimantan and Copeton diamonds must have been extracted from the mantle at a similar time in order for them to plot on the same isotherm. We find that a mantle extraction age of 150–5 Ma (i.e., mid Mesozoic to late Tertiary) for the Kalimantan and Copeton diamonds would be within the uncertainty limits of the T_{NA} data, provided the mantle residency period exceeded about 1 Ga.

Kalimantan diamonds. The possibility of a common lithospheric diamond source now geographically dispersed can be explored in the light of recent paleotectonic reconstructions of the Australasian (i.e., northeastern Gondwanaland) region during the Phanerozoic. In the Paleozoic and early Mesozoic, the tectonic setting of this region was dominated by the separation of microcontinental fragments from the northern Gondwanaland margin. Some of these fragments were incorporated as "exotic" terranes on the south and southeastern margin of the Asian continent (Barber, 1985; Burrett and Stait, 1987; Metcalfe, 1988; Audley-Charles, 1988). The so-called Sundaland continental core of southeast Asia is composed of Gondwanaland fragments that amalgamated with Asia during the Mesozoic (Metcalfe, 1988). It comprises the Sibumasu or Shan-Thai block (Peninsula Malaysia, Thailand, eastern Burma, Sumatra), the East Malaya

block, the Indochina block, and the West Borneo block (which includes the known diamond provinces of Kalimantan). The Indochina and West Borneo blocks were probably connected prior to the opening of the South China Sea in the Tertiary.

There is much evidence to indicate that the Sibumasu terrane of western Sundaland was contiguous with northwest Australia in pre-Permian times (Burrett and Stait, 1985, 1986). The presence of detrital diamonds in Carboniferous sediments of glacial origin in Thailand was originally used as evidence by Ridd (1971) for placement of southeast Asia against India—the only regional diamond source then known. The subsequent discovery of diamondiferous rocks in the Kimberley region, which in addition to the Argyle and Ellendale lamproite pipes include highly eroded diamondiferous kimberlites in the North and East Kimberley regions (Atkinson et al., 1984; Jaques et al., 1986), is now consistent with Australia being that diamond source.

The eastern terranes of Sundaland (Indochina and West Borneo) are thought to have separated from the northern Gondwanaland margin in the early Paleozoic, well before the separation of Sibumasu from Australia (Metcalfe, 1988). It is unlikely, therefore, that the Kalimantan diamonds have a detrital source related to Permo-Carboniferous glaciation of the Australian hinterland. Instead, the coincidence of diamonds on the isotherm in Figure 10 suggests that the Kalimantan diamonds are derived from local primary sources that sampled remnant Gondwanaland subcontinental lithosphere sometime during the mid Mesozoic to Tertiary. This implies that West Borneo (and the originally adjoined Indochina block) was contiguous with northwest Australia in Precambrian times.

We speculate that common diamondiferous lithosphere of a large northeastern Gondwanaland cratonic region may have underlain parts of northern Australia and the proto-southeast Asian blocks in Precambrian times. The present Kimberley block may be a remnant of this larger region. During the Paleozoic, continental fragments bearing this ancient lithosphere were incorporated into southeast Asia. Migration of these fragments evidently did not result in destruction of their lithospheric diamond content (e.g., by lithosphere delamination) as has been proposed by Haggerty (1986) to explain the diamond-poor nature of South American cratons. One might expect, however, that some of the diamond population would record evidence of thermal and mechanical changes associated with continental breakup and migration. The presence of an irregular diamond with high T_{NA} among the Kalimantan alluvials is consistent with this interpretation.

There is some independent evidence to suggest that remnant subcontinental lithosphere may exist beneath the southeast Asian region. In the Sunda Arc region, south of Kalimantan, arc volcanic rocks of ultrapotassic affinity are abundant. Their curious distribution and geochemistry (which have certain similarities with the lamproites of northwestern Australia) led Varne (1985) to postulate on origin for these rocks involving the melting of an ancient Gondwanaland continental lithospheric component. Similarly in the Indochina and West Borneo blocks the occurrence of unusual potassic intrusives and volcanics (cocites and kajanites), that have affinities to minettes and lamproites (Bergman et al., 1988, Wagner and Velde, 1986; Wagner, 1986), may also indicate the presence of Gondwanaland lithosphere with characteristics similar to the source region of lamproites in northwestern Australia. These observations are consistent with the view of Bergman et al. (1987) that lamproite is the most likely primary source for some of the Kalimantan diamonds.

Copeton diamonds of eastern Australia. The occurrence of alluvial diamond deposits in the fold-belt terranes of eastern Australia is enigmatic. This region was part of the active orogenic margin of eastern Gondwanaland during the Paleozoic and Mesozoic (Wyborn, 1989) and was the focus for extensive basaltic volcanism accompanied by elevated geothermal gradients during the Tertiary (O'Reilly and Griffin, 1985). This tectonic environment is clearly not conducive to diamond formation and preservation as conventionally understood (i.e., the association of diamond with thick, cool cratonic lithosphere) yet alluvial diamond deposits are known from throughout the region (MacNevin, 1977; Lishmund and Oakes, 1989). An important question is whether there is a role for Precambrian subcontinental lithosphere in the generation of the eastern Australian diamonds.

The New England Fold Belt, in which the Copeton diamonds occur, is a complex Paleozoic continental-margin accretionary domain composed of various microcontinental fragments, none of which is believed to be of particularly exotic derivation (Cawood and Leitch, 1985). No Precambrian crustal rocks are known from the New England Fold Belt. The adjacent, early Paleozoic Lachlan and Thomson Fold Belts, however, include a number of Precambrian blocks that are thought to have been dispersed as microcontinents during the Proterozoic (Scheibner, 1985). Although parts of eastern Australia are built on ancient lithosphere, much of the original Precambrian crustal history is obscure because of more recent tectonic overprinting.

The occurrence of a portion of the low-N Copeton diamonds on the isotherm at T_{NA} = 1145 °C, common to West Kimberley and Kalimantan lithospheres, suggests that Copeton diamonds occurred in ancient lithosphere of northeastern Gondwanaland derivation. This implies either (1) that Precambrian lithosphere may underlie parts of the New England Fold Belt but has no crustal expression or (2) that the Copeton source is not local but is derived from a Precambrian block farther to the west. Because of the similarities between Copeton and Kalimantan diamonds, we favor the former interpretation. The absence of platelet-degraded diamonds among the Copeton stones, however, argues against a Copeton litho-

spheric source that has experienced a prolonged migratory history following diamond incorporation; a northern Australian source for this lithosphere seems likely.

The diamonds belonging to the isotherm at 1145 °C are postulated to be of Proterozoic age and peridotitic affinity by analogy with the Ellendale-9 diamonds. The majority (>80%) of the Copeton diamonds are, however, of eclogitic parentage and have a range of T_{NA} values (Fig. 10) reflecting differing depths of origin within the lithosphere or different times of diamond formation. It is not possible with the present data to decide whether diamonds constrained to these isotherms correspond to different primary volcanic pipe sources. Since there are as yet no detailed age constraints on formation of the Copeton eclogitic diamonds, an age range from early Proterozoic to Mesozoic can be inferred.

To generate the required degree of N aggregation among the eclogitic Copeton diamonds, the lithosphere must have been within the diamond stability field for at least 20 Ma for storage temperatures as high as 1300 °C and considerably longer for lower temperature storage (see Fig. 9). If the eclogite source is subducted crust, then this crust must have been stabilized (i.e., anchored) by attachment to rigid lithosphere for a long period. This precludes models for the origin of Copeton diamonds involving rapid uplift of newly subducted, cold eclogitic crust or obduction of cold ophiolite peridotite (e.g., Nixon and Bergman, 1987) in a collisional arc environment. A deeply subducted source is also not possible, since pyroxene solid solution is absent from garnet inclusions in Copeton diamonds (Sobolev, 1984), limiting the source region to a depth of less than 250 km (~7.5 GPa) (Irifune et al., 1989).

The distinctive heavy $\delta^{13}C$ values of Copeton eclogitic diamonds (~0 to +2‰), combined with the unusual coesite-rich and Al_2O_3-undersaturated (i.e., kyanite-absent) nature of the inclusion suite (which is atypical of other calcic inclusion suites such as grospydites), is evidence for the involvement of crustal carbon (marine carbonates?) and siliceous calc-silicates in their genesis. Clinopyroxene inclusions analyzed by Sobolev (1984) range from magnesian (Mg no. 98.2), low Al_2O_3, Na_2O compositions, having affinity with diopsides found in calc-silicate metasediments, to omphacitic pyroxenes more typical of basaltic derivation. These observations led Sobolev (1984) to postulate a volcanogenic-sedimentary protolith, although saussuritized (i.e., Ca-metasomatized) gabbros, formed by hydrothermal alteration, may also be suitable protoliths, provided the bulk compositions are sufficiently silica-rich.

The high N content of the yellow Copeton diamonds is of interest, since eclogite protoliths (i.e., basalts, gabbros, and their hydrothermally altered equivalents) are strongly N depleted (containing <1–10 ppm N: Wlotzka, 1972; Hall, 1988) and deep-mantle N sources (e.g., Javoy et al., 1984; Boyd et al., 1987) are unlikely contributors in view of the strictly crustal $\delta^{13}C$ signature of Copeton diamonds. A possible N source for these diamonds is crustally derived N carried into the diamond stability field as a component of phlogopitic mica with $NH_4 \leftrightarrow K$ substitution, the volatile nitrogenous component being released on phlogopite decomposition at ~6.5 GPa (Tatsumi, 1989). This tends to favor a role for metasedimentary rather than metaigneous calc-silicates, since magnesian phlogopite, with the necessary high-pressure stability, is a common accessory phase in calc-silicate metasediments.

For the Copeton eclogitic diamonds, a subduction-related, recycled crustal source including basaltic and siliceous calc-silicate elements accreted onto old, remnant microcontinental lithosphere derived from northeastern Gondwanaland margin appears most likely. Because the elevated geothermal gradients that prevailed during the Tertiary in eastern Australia (O'Reilly and Griffin, 1985) would have generated conditions unsuitable for diamond survival at depth, and noting the N aggregation constraints discussed above, we favor a volcanic pipe (or pipes) of mid-to late Mesozoic age as the primary source.

Concluding remarks and future applications

We have demonstrated that the N aggregation characteristics of diamond can be used to identify distinct time-temperature populations among pipe and alluvial diamonds. These features reflect the nature and evolution of the lithospheric source. In the case of the Kimberley lithosphere the picture of diamond distribution in space and time is shown to be more complex than the idealized model of Haggerty (1986). We have shown that formation of the Australasian diamonds is not restricted to one particular time interval, and therefore a regular distribution of A/B defect ratios with lithospheric depth of the diamond source is not necessarily valid. Furthermore, we have shown that N content of diamond is not useful as an indicator of paragenetic association, since eclogitic diamonds as well as those of peridotitic affinity can have a large range of N contents. A similar conclusion was also reached by Deines et al. (1989) from studies of Premier and Finsch diamonds. In eclogitic diamonds, high N contents presumably reflect N input from deep-mantle sources (e.g., Ellendale-4 diamonds) or recycled sedimentary sources (e.g., Copeton high-N group), whereas low N contents (e.g., Argyle) reflect the N-improverished nature of recycled basaltic crust. N contents may also be influenced by the nature of the crystallization environment, particularly temperature and f_{O_2} (Deines et al., 1989).

An important implication of this study is that diamond may persist in dispersed microcontinental lithosphere despite the extensive lithosphere thinning that must accompany continental fragmentation. In cases such as Kalimantan and Copeton, where the oldest local crustal rocks are Paleozoic, the crust may be effectively decoupled from an underlying older lithospheric diamond source region.

The Australasian diamonds do not conform to the general observation that peridotitic diamonds have formed

and evolved at lower temperatures than eclogitic diamonds (e.g., Gurney, 1989). Since problems with calibration of the silicate geothermometers and uncertainty in pressure estimates may contribute to the observed temperature difference between peridotitic and eclogitic suites, it would be of value to use N aggregation data to investigate this trend in a large number of samples.

We have shown that a diamond population can be characterized by its N content, extent of aggregation of A defects (T_{NA} value for a known or assumed t_{MR}), and platelet degradation state; the last mentioned is sensitive to thermomechanical events in the host lithosphere and may be indicative of contintental rifting or migration. Thus diamond should prove effective as a tracer in paleotectonic reconstructions (as discussed above), in provenance studies of alluvial or detrital diamonds, and in deducing the thermal evolution of continental lithosphere, particularly when combined with additional geothermometric and geochronological data. In applications to diamond provenance, source characteristics of a statistically significant sample of alluvial diamonds may be compared with known primary diamonds, thus allowing identification of unrecognized contributory sources. The degree of uniformity in spatial distribution of diamond populations within an alluvial field may also be of value in deciding whether local or distal diamond sources are involved.

A useful future application will be in understanding the relationships among microdiamonds, macrodiamonds, and their host magma. Preliminary studies of cubic microdiamonds from northern Australia using IR microscopy show that they contain 100% A defects with no platelet development. These features are consistent with short-term mantle storage and the possibility of magmatic crystallization (cf. Boyd et al., 1987).

Acknowledgments

We gratefully acknowledge Argyle Diamond Mines Ltd. and the Ashton Joint Venture for the provision of Argyle and Ellendale stones and the following individuals for provision of diamond samples: A.C.T. Joris (Copeton CO series), A.C. Goode and W.L. Griffin (Copeton DA series), and P.E. Pieters (Kalimantan). We also thank C.B. Smith, S.E. Kesson, R. Ramsay, and two anonymous referees for helpful comments on the manuscript, and P.E. Pieters and D. Trail for information on Kalimantan geology. T. Mernagh kindly carried out analyses of inclusions by laser Raman microprobe. This study was supported by an Australian National Research Fellowship (held by W.R.T. at the University of Tasmania), and a University of Western Australia Postdoctoral Fellowship and Australian Research Council funding to D.H. Green (University of Tasmania). A.L.J. publishes with the permission of the Executive Director, Bureau of Mineral Resources, Geology, and Geophysics.

References cited

Allen, B.P., and Evans, T. (1981) Aggregation of nitrogen in diamond including platelet formation. Proceedings of the Royal Society London, A375, 93–104.

Atkinson, W.J. (1989) Diamond exploration philosophy, practise and promises: A review. In J. Ross et al., Eds., Kimberlites and related rocks, vol. 2, Geological Society of Australia Special Publication no. 14, p. 1075–1107. Blackwell Scientific Publications, Melbourne.

Atkinson, W.J., Hughes, F.E., and Smith, C.B. (1984) A review of the kimberlitic rocks of Western Australia. In J. Kornprobst, Ed., Kimberlites and related rocks, vol. 1, Proceedings of the Third International Kimberlite Conference, p. 195–224. Elsevier, Amsterdam.

Audley-Charles, M.G. (1988) Evolution of the southern margin of Tethys (north Australian region) from early Permian to late Cretaceous. In M.G. Audley-Charles and A. Hallam, Eds., Gondwana and Tethys, Geological Society Special Publication no. 37, p. 79–100. Geological Society, London.

Barber, A.J. (1985) The relationship between the tectonic evolution of southeast Asia and hydrocarbon occurrences. In D.G. Howell, Ed., Tectonostratigraphic terranes of the Circum-Pacific Region, p. 523–528. Cirum-Pacific Council for Energy and Mineral Resources, Houston, Texas.

Bardet, M.G. (1977) Geologie du Diamant, Bureau de Recherches Geologiques et Mineres Memoir, 83, III.

Barry, J.C., Bursill, L.A., and Hutchison, J.L. (1985) On the structure of {100} platelet defects in type Ia diamond. Philosophical Magazine, A51, 15–49.

Bergman, S.C., Turner, W.S., and Krol, L.G. (1987) A reassessment of the diamondiferous Pamali Breccia, southeast Kalimantan, Indonesia: Intrusive kimberlite breccia or sedimentary conglomerate? In E.M. Morris and J.D. Pasteris, Eds., Mantle metasomatism and alkaline magmatism, Geological Society of America Special Paper 215, p. 183–195.

Bergman, S.C., Dunn, D.P., and Krol, L.G. (1988) Rock and mineral chemistry of the Linhaisai Minette, Central Kalimantan, Indonesia, and the origin of Borneo Diamonds. Canadian Mineralogist, 26, 23–43.

Bibby, D.M. (1982) Impurities in natural diamond. In P.A. Thrower, Ed., Chemistry and physics of carbon, vol. 18, p. 1–91. Marcel Dekker, New York.

Boyd, S.R., Mattey, D.P., Pillinger, C.T., Milledge, H.J., Mendelssohn, M., and Seal, M. (1987) Multiple growth events during diamond genesis: An integrated study of carbon and nitrogen isotopes and nitrogen aggregation state in coated stones. Earth and Planetary Science Letters, 86, 341–353.

Brey, G.P. (1989) Geothermometry for Iherzolites: Experiments from 10 to 60 kbar, new geothermometers, and application to natural rocks. Habilitations Thesis, Mineralogisches Institut, University of Darmstadt, (unpublished). Darmstadt, Germany.

Brozel, M.R., Evans, T., and Stephenson, R.F. (1978) Partial dissociation of nitrogen aggregates in diamond by high temperature–high pressure treatments. Proceedings of the Royal Society London, A361, 109–127.

Burrett, C., and Stait, B. (1985) South East Asia as a part of an Ordovician Gondwanaland—A palaeobiogeographic test of a tectonic hypothesis. Earth and Planetary Science Letters, 75, 184–190.

——— (1986) Southeast Asia as a part of an early Palaeozoic Australian Gondwanaland. Geological Society of Malaysia Bulletin, 19, 103–107.

——— (1987) China and southeast Asia as part of the Tethyan margin of Cambro-Ordovician Gondwanaland. In K.G. McKenzie, Ed., Proceedings of the International Symposium on Shallow Tethys 2, p. 65–77. A.A. Balkema, Rotterdam.

Bursill, L.A. (1983) Small and extended defect structures in gem-quality Type I diamonds. Endeavour (New Series), 7, 70–77.

Bursill, L.A., and Glaisher, R.W. (1985) Aggregation and dissolution of small and extended defect structures in Type Ia diamond. American Mineralogist, 70, 608–618.

Cawood, P.A., and Leitch, E.C. (1985) Accretion and dispersal tectonics of the southern New England fold belt, eastern Australia. In D.G. Howell, Ed., Tectonostratigraphic terranes of the Circum-Pacific Region, p. 481–492. Cirum-Pacific Council for Energy and Mineral Resources, Houston, Texas.

Chrenko, R.M., McDonald, R.S., and Darrow, K.A. (1967) Infra-red spectra of diamond coat. Nature, 213, 474–476.

Chrenko, R.M., Tuft, R.E., and Strong, H.M. (1977) Transformation of the state of nitrogen in diamond. Nature, 270, 141–144.

Clark, C.D., and Davey, S.T. (1984a) One-phonon infrared absorption in diamond. Journal of Physics C: Solid State Physics, 17, 1127–1140.

——— (1984b) Defect-induced one-phonon absorption in type Ia diamonds. Journal of Physics C: Solid State Physics, 17, L399–L403.

Davies, G. (1976) The A nitrogen aggregate in diamond—its symmetry and possible structure. Journal of Physics C, 9, L537–L542.

Davies, G. (1981) Decomposing the IR absorption spectra of diamonds. Nature, 290, 40–41.

Deines, P. (1980) The carbon isotopic composition of diamonds: Relationship to diamond shape, color, occurrence and vapor composition. Geochimica et Cosmochimica Acta, 44, 943–961.

Deines, P., Harris, J.W., Spear, P.M., and Gurney, J.J. (1989) Nitrogen and ^{13}C content of Finsch and Premier diamonds and their implications. Geochimica et Cosmochimica Acta, 53, 1367–1378.

Dyer, H.B., Raal, F.A., duPreez, L., and Loubser, J.H.N. (1965) Optical absorption features associated with paramagnetic nitrogen in diamond. Philosophical Magazine, 11, 763–774.

Evans, T., and Harris, J.W. (1989) Nitrogen aggregation, inclusion equilibration temperatures and the age of diamonds. In J. Ross et al., Eds., Kimberlites and related rocks, vol. 2, Geological Society of Australia Special Publication no. 14, p. 1001–1006. Blackwell Scientific Publications, Melbourne.

Evans, T., and Qi, Z. (1982) The kinetics of the aggregation of nitrogen atoms in diamond. Proceedings of the Royal Society London, A381, 159–178.

Green, D.H., Falloon, T.J., and Taylor, W.R. (1987) Mantle-derived magmas—Roles of variable source peridotite and variable C-H-O fluid compositions. In B.O. Mysen, Ed., Magmatic processes: Physicochemical principals. Geochemical Society Special Publication no. 1, p. 139–154, The Geochemical Society, Pennsylvania.

Griffin, W.L., Jaques, A.L., Sie, S.H., Ryan, C.G., Cousens, D.R., and Suter, G.F. (1988) Conditions of diamond growth: A proton microprobe study of inclusions in West Australian diamonds. Contributions to Mineralogy and Petrology, 99, 143–158.

Gurney, J.J. (1989) Diamonds. In J. Ross et al., Eds., Kimberlites and related rocks, vol. 2, Geological Society of Australia Special Publication no. 14, p. 935–965. Blackwell Scientific Publications, Melbourne.

Hall, A. (1988) Crustal contamination of minette magmas: Evidence from their ammonium contents. Neues Jahrbuch für Mineralogie Monatshefte, 137–143.

Hall, A.E., and Smith, C.B. (1984) Lamproite diamonds—Are they different? In J.E. Glover and P.G. Harris, Eds., Kimberlite occurrence and origin: A basis for conceptual models in exploration, University Extension Publication no. 8, p. 167–212. The University of Western Australia.

Haggerty, S.E. (1986) Diamond genesis in a multiply-constrained model. Nature, 320, 34–37.

Harris, J.W. (1987) Recent physical, chemical and isotopic research of diamond. In P.H. Nixon, Ed., Mantle xenoliths, p. 477–500. Wiley, Chichester, England.

Harris, J.W., and Collins, A.T. (1985) Studies of Argyle diamonds. Industrial Diamond Review, 45, 128–130.

Helmstaedt, H., and Gurney, J.J. (1984) Kimberlites of southern Africa—Are they related to subduction processes? In J. Kornprobst, Ed., Kimberlites and related rocks, vol. 1, Proceedings of the Third International Kimberlite Conference, p. 425–434. Elsevier, Amsterdam.

Helmstaedt, H., and Schulze, D.J. (1989) Southern African kimberlites and their mantle sample: Implications for Archaean tectonics and lithosphere evolution. In J. Ross et al., Eds., Kimberlites and related rocks, vol. 1, Geological Society of Australia Special Publication no. 14, p. 358–368. Blackwell Scientific Publications, Melbourne.

Holloway, J.R., and Wood, B.J. (1988) Simulating the Earth—Experimental Geochemistry, 196 pp. Unwin Hyman, Boston.

Humble, P. (1982) The structure and mechanism of formation of platelets in natural type Ia diamond. Proceedings of the Royal Society London, A381, 65–81.

Irifune, T., Hibberson, W.O., and Ringwood, A.E. (1989) Eclogite-garnetite transformation at high pressure and its bearing on the occurrence of garnet inclusions in diamond. In J. Ross et al., Eds., Kimberlites and related rocks, vol. 2, Geological Society of Australia Special Publication no. 14, p. 877–882. Blackwell Scientific Publications, Melbourne.

Jaques, A.L., Lewis, J.D., Smith, C.B., Gregory, G.P., Ferguson, J., Chappell, B.W., and McCulloch, M.T. (1984) The diamond-bearing ultrapotassic (lamproitic) rocks of the West Kimberley region, Western Australia. In J. Kornprobst, Ed., Kimberlites and related rocks, vol. 1, Proceedings of the Third International Kimberlite Conference, p. 225–255. Elsevier, Amsterdam.

Jaques, A.L., Lewis, J.D., and Smith, C.B. (1986) The kimberlitic and lamproitic rocks of Western Australia. Geological Survey of Western Australia Bulletin, 132, 268 p.

Jaques, A.L., Hall, A.E., Sheraton, J.W., Smith, C.B., Sun S-S, Drew, R.M., Foudoulis, C., and Ellingsen, K. (1989) Composition of crystalline inclusions and C-isotopic composition of Argyle and Ellendale diamonds. In J. Ross et al., Eds., Kimberlites and related rocks, vol. 2, Geological Society of Australia Special Publication no. 14, p. 966–989. Blackwell Scientific Publications, Melbourne.

Jaques A.L., O'Neill, H.St.C, Smith, C.B., Moon, J., and Chappell, B.W. (1990) Diamondiferous peridotite xenoliths from the Argyle (AK1) lamproite pipe, Western Australia. Contributions to Mineralogy and Petrology, 104, 255–276.

Javoy, M., Pineau, F., and Demaiffe, D. (1984) Nitrogen and carbon isotopic composition in the diamonds of Mbuji Mayi (Zaire). Earth and Planetary Science Letters, 68, 399–412.

Joris, A.C.T. (1983) Some uncuttable diamonds from New South Wales, Australia. Indiaqua, 36, 41–43.

Kaiser, W., and Bond, W.L. (1959) Nitrogen, a major impurity in common type I diamond. Physical Review, 115, 857–863.

Kesson, S.E., and Ringwood, A.E. (1989) Slab-mantle interactions 2. The formation of diamonds. Chemical Geology, 78, 97–118.

Kramers, J.D. (1979) Lead, uranium, strontium, potassium and rubidium in inclusion-bearing diamond and mantle-derived xenoliths from southern Africa. Earth and Planetary Science Letters, 42, 58–70.

Lang, A.R. (1979) In J.E. Field, Ed., The properties of diamond, chapter 16, p. 425–469. Academic Press, London.

Lishmund, S.R., and Oakes, G.M. (1989) Gemstones. In R.W. Johnson, Ed., Intraplate volcanism in eastern Australia and New Zealand, p. 152–155. Cambridge University Press, Cambridge, England.

MacGregor, I.D., and Manton, W.I. (1986) Roberts Victor eclogites: Ancient oceanic crust. Journal of Geophysical Research, 91, 14063–14079.

MacNevin, A.A. (1977) Diamonds of New South Wales. Mineral Resources Report, 42, Department of Mines, Geological Survey of New South Wales.

Metcalfe, I. (1988) Origin and assembly of south-east Asian continental terranes. In M.G. Audley-Charles and A. Hallam, Eds., Gondwana and Tethys, Geological Society Special Publication no. 37, p. 101–118. Geological Society, London.

Meyer, H.O.A. (1985) Genesis of diamond: A mantle saga. American Mineralogist, 70, 344–355.

Milledge, H.J., Mendelssohn, M.J., Boyd, S.R., Pillinger, C.T., and Seal, M. (1989) Infrared topography and carbon and nitrogen isotope distribution in natural and synthetic diamonds in relation to mantle processes. In Extended Abstracts, Workshop on diamonds, 28th International Geological Congress, Washington, D.C., p. 55–60.

Nixon, P.H., and Bergman, S.C. (1987) Anomalous occurrences of diamonds. Indiaqua, 47, 21–27.

O'Reilly, S.Y., and Griffin, W.L. (1985) A xenolith-derived geotherm for south-eastern Australia and its geophysical implications. Tectonophysics, 111, 41–63.

Phillips, D., Onstott, T.C., and Harris, J.W. (1989) $^{40}Ar/^{39}Ar$ laser-probe dating of diamond inclusions from the Premier kimberlite. Nature, 340, 460–462.

Pidgeon, R.T., Smith, C.B., and Fanning, C.M. (1989) Kimberlite and lamproite emplacement ages in Western Australia. In J. Ross et al., Eds., Kimberlites and related rocks, vol. 1, Geological Society of Australia Special Publication no. 14, p. 369–381. Blackwell Scientific Publications, Melbourne.

Pohkilenko, N.P., and Sobolev, N.V. (1986) Xenoliths of diamondiferous peridotites from Udachnaya kimberlite, Yakutia. In Extended Abstracts, 4th International Kimberlite Conference, Geological Society of Australia Abstracts no. 16, p. 309–311.

Richardson, S.H. (1986) Latter-day origin of diamonds of eclogitic paragenesis. Nature, 322, 623–626.

Richardson, S.H., Gurney, J.J., Erlank, A.J., and Harris, J.W. (1984) Origin of diamonds in old enriched mantle. Nature, 310, 198–202.

Ridd, M.F. (1971) Southeast Asia as a part of Gondwanaland. Nature, 234, 531–533.

Runciman, W.A., and Carter, T. (1971) High Resolution infra-red spectra of diamond. Solid State Communications, 9, 315–317.

Scheibner, E. (1985) Suspect terranes in the Tasman fold belt system, eastern Australia. In D.G. Howell, Ed., Tectono-stratigraphic terranes of the Circum-Pacific Region, p. 493–514. Cirum-Pacific Council for Energy and Mineral Resources, Houston, Texas.

Seal, M. (1965) Structure in diamonds as revealed by etching. American Mineralogist, 50, 105–131.

Shee, S.R., Gurney, J.J., and Robinson, D.N. (1982) Two diamond-bearing peridotite xenoliths from the Finsch Kimberlite, South Africa. Contribution to Mineralogy and Petrology, 81, 79–87.

Smith, S.D., and Taylor, W. (1962) Optical phonon effects in the infrared spectrum of acceptor centres in semiconducting diamond. Proceedings of the Physical Society, 79, 1142–1153.

Smith, C.B., Gurney, J.J., Harris, J.W., Robinson, D.N., Shee, S.R., and Jagoutz, E. (1989) Sr and Nd isotopic systematics of diamond-bearing eclogite xenoliths and eclogitic inclusions in diamond from southern Africa. In J. Ross et al., Eds., Kimberlites and related rocks, vol. 2, Geological Society of Australia Special Publication no. 14, p. 853–863. Blackwell Scientific Publications, Melbourne.

Sobolev N.V. (1984) Crystalline inclusions in diamonds from New South Wales, Australia. In J.E. Glover and P.G. Harris, Eds., Kimberlite occurrence and origin: A basis for conceptual models in exploration, University Extension Publication no. 8, p. 213–226. The University of Western Australia.

Sobolev, N.V., Galimov, E.M., Ivanovskaya, N.N., and Yefimova, E.S. (1979) Isotopic composition of the carbon from diamonds containing inclusions. Doklady Akademii Nauk SSSR, 249, 1217–1220 (in Russian).

Spera, F.J. (1984) Carbon dioxide in igneous petrogenesis. III. Role of volatiles in the ascent of alkaline magma with special reference to xenolith-bearing mafic lavas. Contributions to Mineralogy and Petrology, 74, 55–66.

Swart, P.K., Pillinger, C.T., Milledge, H.J., and Seal, M. (1983) Carbon isotopic variation within individual diamonds. Nature, 303, 793–795.

Tatsumi, Y. (1989) Migration of fluid phases and genesis of basaltic magmas in subduction zones. Journal of Geophysical Research, 94, 4697–4707.

Taylor, W.R., and Green, D.H. (1988) Measurement of reduced peridotite-C-O-H solidus and implications for redox melting of the mantle. Nature, 332, 349–352.

——— (1989) The role of reduced C-O-H fluids in mantle partial melting. In J. Ross et al., Ed., Kimberlites and related rocks, vol. 1, Geological Society of Australia Special Publication no. 14, p. 592–602. Blackwell Scientific Publications, Melbourne.

Varne, R. (1985) Ancient subcontinental mantle: a source for K-rich orogenic volcanics. Geology, 13, 405–408.

Wagner, C. (1986) Mineralogy of the type kajanite from Kalimantan. Similarities and differences with typical lamproites. Bulletin de Minéralogie, 109, 589–598.

Wagner, C., and Velde, D. (1986) Lamproites in North Vietnam? A re-examination of "cocites." Journal of Geology, 94, 770–776.

Wlotzka, F. (1972) Nitrogen abundance in common igneous rock types. In K.H. Wedepohl, Ed., Handbook of geochemistry, section 7-E. Springer-Verlag, Berlin.

Woods, G.S. (1986) Platelets and the infrared absorption of type Ia diamonds. Proceedings of the Royal Society London, A407, 219–238.

Woods, G.S., and Collins, A.T. (1983) Infrared absorption spectra of hydrogen complexes in type I diamonds. Journal of Physics and Chemistry of Solids, 44, 471–475.

Wyborn, D. (1989) Geology of eastern Australia. In R.W. Johnson, Ed., Intraplate volcanism in eastern Australia and New Zealand, p. 18–21. Cambridge University Press, Cambridge, England.

Manuscript received January 15, 1990
Manuscript accepted October 2, 1990